Mental search of concepts is supported by egocentric vector representations and restructured grid maps

Simone Viganò[1,2,†], Rena Bayramova[1], Christian F. Doeller[1,3,4*], Roberto Bottini[2,*,†]

[1] Max Planck Institute for Human Cognitive and Brain Sciences, Leipzig, Germany

[2] Center for Mind/Brain Sciences, University of Trento, Rovereto, Italy

[3] Kavli Institute for Systems Neuroscience, Center for Neural Computation, The Egil and Pauline Braathen and Fred Kavli Center for Cortical Microcircuits, Jebsen Center for Alzheimer's Disease, Norwegian University of Science and Technology, Trondheim, Norway

[4] Wilhelm Wundt Institute of Psychology, Leipzig University, Leipzig, Germany.

[*] co-senior authors

[†] corresponding authors: S Viganò simone.vigano@unitn.it ; R Bottini roberto.bottini@unitn.it

Abstract

The human hippocampal-entorhinal system is known to represent both spatial locations and abstract concepts in memory in the form of allocentric cognitive maps. Using fMRI, we show that the human parietal cortex evokes complementary egocentric-like vector representations in conceptual spaces during goal-directed mental search, akin to those observable during physical navigation to determine where a goal is located relative to oneself. Concurrently, grid-like representations, a neural signature of allocentric cognitive maps in entorhinal, prefrontal, and parietal cortices, are restructured as a function of conceptual goal proximity, akin to rodent grid cells firing around reward locations during spatial exploration. These brain mechanisms might support flexible and parallel readout of where target conceptual information is stored in memory, capitalizing on complementary reference frames.

Introduction

One of the hallmarks of our species is the ability to store and manipulate the knowledge we have about the world, and to organize concepts and memories for later retrieval. Cognitive (neuro)scientists have proposed that humans organize their world knowledge in "cognitive maps" [1,2], internal models of how memories relate to each other [3-6]. The hippocampal-entorhinal system in the medial temporal lobe of mammals contains spatially modulated neurons, such as place cells [7] or grid cells [8] that, by selectively firing when the animal is at a specific location in the environment, provide a neural basis for cognitive maps of their surroundings. Functional magnetic resonance imaging (fMRI) in humans has revealed that similar coding schemes in the same brain regions and in the medial prefrontal cortex can be detected non-invasively while participants are engaged in virtual reality navigation tasks [9-11] and also when, in more abstract decision-making, they need to process relational knowledge between non-spatial stimuli, such as visual shapes or objects [12-13], odors [14], people's identities [15], or word meanings [16-17]. This supports the proposal of a phylogenetic continuity between spatial navigation abilities and memory in humans [18]: the brain circuits that evolved for navigating physical spaces in other mammals might be used in our species for organizing conceptual knowledge, enabling us to "mentally navigate" through concepts and memories as if they were locations in our internal conceptual spaces [3,6,19]. However, the human navigation system goes well beyond hippocampal cognitive maps. During physical navigation in real and virtual environments, wayfinding and spatial self-localization is performed by means of the parallel recruitment of complementary reference frames: *allocentric* representations (indeed associated with the hippocampal formation) encode objects position in relationship with other objects, stable landmarks or environmental geometry; on the other hand, *egocentric* representations (usually associated with parietal regions) encode object position with respect to the observer's perspective, and changes as a function of the observer's movements [20-22]. It has been hypothesized that complementary allocentric and egocentric reference frames may be recruited also during the exploration of conceptual spaces [6], suggesting a repurposing of the wider human navigation network (hippocampal-parietal system) for conceptual 'navigation', but empirical evidence to date is still missing.

Here we test this hypothesis by investigating how the human brain represents and guides the retrieval of relevant goal information in conceptual spaces during mental search. Indeed, when looking for specific goal objects or locations during physical navigation, both egocentric and allocentric mechanisms guide our search in the environment. First, egocentric or viewpoint-dependent representations allow us to tell whether an object is, at a specific moment in time, to our left, right, front, or back, thus providing information about its location relative to our current position or movement trajectory (that is, our current state). The neural circuits supporting this egocentric coding rely mainly on the parietal cortex, as confirmed by neuropsychology [23-25], functional neuroimaging [26-29], and neurophysiology [30-31]. Second, goals can also be tracked by altering and restructuring the allocentric cognitive maps in the hippocampal formation: goal locations are indeed overrepresented by spatially tuned neurons compared to more distant regions of space [32], as it happens for instance with entorhinal grid cell fields, that expand and shift towards goals [33] and are more densely packed at the goal location [33,34]. Is it possible that specific goal information in conceptual spaces elicit similar neural effects across different reference frames? Do they evoke egocentric-like coding schemes when we look for them in memory, to orient and guide our

mental search? Do they alter the allocentric cognitive map to signal their position in conceptual space?

To answer these questions, we designed an experiment where human participants had to retrieve conceptual goals in simple, but highly controlled feature spaces, allowing us to monitor their brain activity as a function of their "mental search". We instructed 40 adult volunteers to imagine being scientists in a future society where humankind lives in peace and prosperity thanks to the development of two (fictitious) molecules, called *Megamind* and *Megabody*, which grant people increased cognitive and physical abilities, respectively. The two molecules that represented the goals were identical for all but two crucial aspects: their color (blue vs green, hereafter referred to as "contexts"), and the specific ratios of their upper and lower bonds (hereafter referred to as "aspect ratio"), see Fig. 1a. Unbeknown to participants, the two molecules were defined as points in 2D feature spaces, with one axis indicating the length of the upper bond and the other one the length of the lower bond (Fig. 1b), see Methods for further details. Participants were told that they were among the scientists recruited to produce these molecules via specific computer-based tasks over the course of 2 days (Fig. 1c). To produce the goal molecules, they had to actively morph feature configurations into the target ones using computer-controlled "reactions" (see Methods), and this was conceivable as navigating the two "molecule spaces" (or contexts) in order to find the conceptually relevant labeled location (our "conceptual goals"), Supplementary Fig. 1a. Then, during a subsequent fMRI session, participants were presented with predetermined reactions, showing morphing molecules whose aspect ratio changed in a predetermined way (that is, following specific trajectories), Fig. 1d. They were asked to imagine the morphing to continue in the same way and to indicate whether or not the reaction would have resulted in the molecule becoming Megamind or Megabody. We predicted that, analogous to spatial navigation, brain activity during abstract conceptual search would convey information about goals locations in feature spaces by exhibiting 1) egocentric-like coding of the conceptual goals, and 2) an alteration of the allocentric cognitive map as a function of goal proximity.
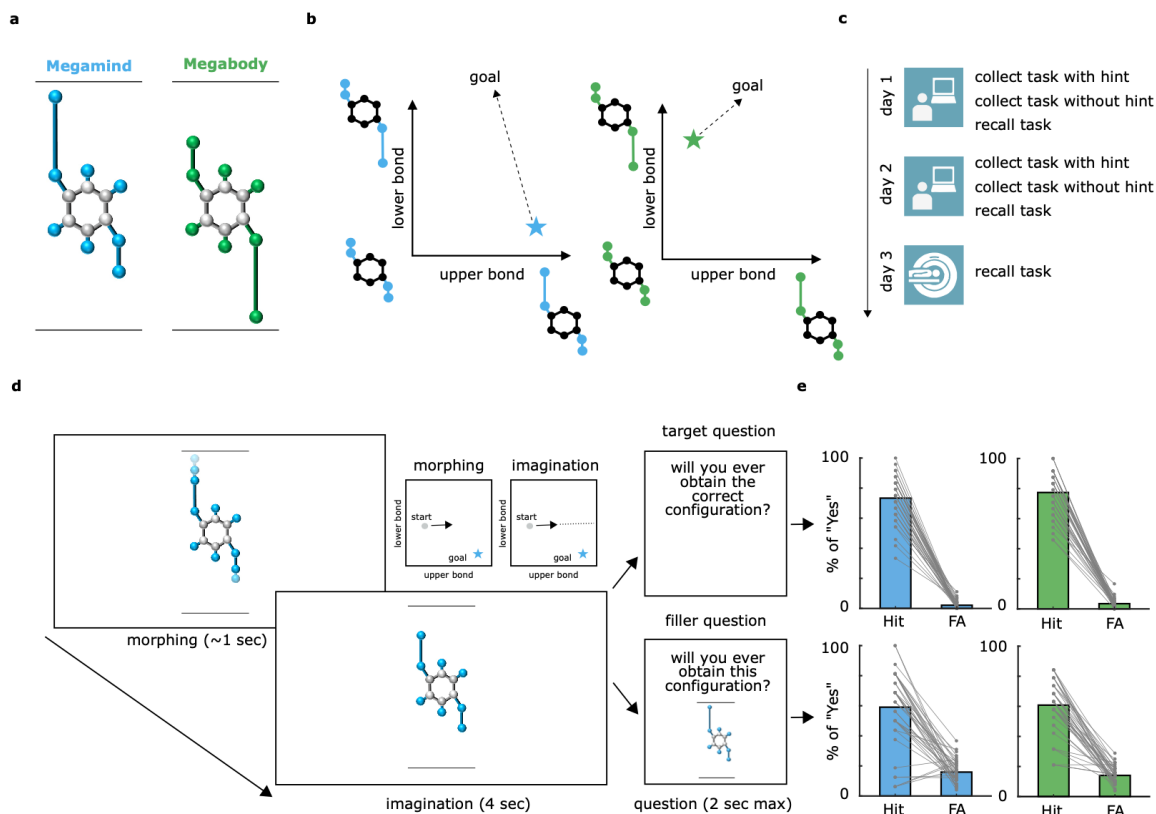
Fig. 1 | Conceptual goals in feature space and experimental design. a, Participants learned about two fictitious goal molecules, named Megamind and Megabody, with their characteristic colors and ratios between the upper and lower bond ("aspect ratio"). **b**, The two goal molecules were conceivable as goal locations in bidimensional feature spaces defined by the length of the two bonds. **c**, The experiment lasted 3 days. During the first 2 days, participants learned how to "produce" the goal molecules by actively morphing feature configurations into the target ones (thus effectively 'navigating' the feature spaces to find goal locations), via a computer-based behavioral training. Further detail on these training tasks and their results are in the Methods section and in Supplementary Figures 1-2-3. On the third and last day, during an fMRI scanning session, participants evaluated some reactions while keeping in mind conceptual goals. **d**, The "Recall task" was performed during training and during fMRI. Participants were prompted with a random feature configuration which started morphing autonomously for about 1 second. After morphing stopped, they had 4 seconds to imagine the morphing to continue in the same way. Then, one of two possible questions appeared. The "Target question" asked whether the goal molecule would ever be obtained if the morphing continued in the same way. The "Filler question" asked whether a specific molecule configuration (different from the goal molecule) shown on the screen will ever be obtained. The bar plots in the right panels show the percentage of hits and false alarms for the two molecules and the two questions on the fMRI day. Performance on the training days is shown in Supplementary Fig. 4-5-6-7. *** p < 0.001

Results

Participants successfully retrieve conceptual goals in feature spaces

Participants were trained for two consecutive days to find the goal molecules in the two contexts: they learned to actively morph wrong molecules into correct ones by modifying their aspect ratio to match either Megamind or Megabody depending on the color context (see Methods and Supplementary Figure 1). Unbeknown to participants, this was conceivable as navigating the molecule space to find goal locations. Participants successfully completed the training, as indicated by the time to finish the tasks, the number of transitions necessary to find the goals and the number of correct molecules collected in a given time window (Supplementary Figure 1 and 2), suggesting that they had learned and memorized how the conceptual goals looked like or, equivalently, where the conceptual goals were located in the two contexts. At the end of each training day and during the fMRI session (day 3), participants performed the "Recall task" (see Methods), consisting of the presentation of a random morphing molecule and of an imagination period (Fig. 1d). Here, participants were instructed to imagine the morphing ("reaction") to continue infinitely in the very same way, and to imagine whether or not the molecule would ever match the goal configuration (that is, in spatial terms, if the trajectory would ever pass through the goal location), which they had learned during training and which they had to keep in mind. This was referred to as the "target question" (Fig. 1d). Critically, the trajectories implied by the morphing molecules could be directed to the goal (0° from correct trajectory; on-target trials, participants are expected to respond "Yes") or deviating from it by a certain degree (-135°, -90°, -45°, +45°, +90° +135° from correct trajectory; off-target trials, the expected response was "No". Signs could be interpreted as arbitrary "left" and "right", see Methods and Supplementary Figure 3): these angular conditions will be referred to as "egocentric-like conditions", because they indicate where the goal is in the feature space with respect to the current trajectory, independently from their allocentric position and from the angle of movement relative to the general layout of the feature space (Fig. 2a). To ascertain that participants were also actively constructing a representation of the entire navigable space, on 50% of the trials, instead of the "target question", we presented a "filler question", where we asked participants to detect whether or not the morphing would have resulted in a specific, randomly chosen, configuration that was different from the goal and that was presented on the screen only for that specific trial (see Methods). Participants did not know in advance the type of question they were going to be presented with and, by analyzing the "imagination period" in our fMRI data, we could address all the main questions of our study without significant influence from the "question period". Participants had a very good performance on both training days: they successfully distinguished correct trajectories from incorrect ones in both the "target questions" (Supplementary Figure 4) and the "filler questions" (Supplementary Figure 6). The analysis of reaction times (RTs) showed only modest differences between correct and incorrect trajectories, mostly in the "filler questions", with on-target trials being recognized slightly more slowly than off-target ones (Supplementary Figure 5 and 7). This task was repeated on the 3rd and last day of the experiment, during the fMRI scanning session (see Methods), where participants maintained their high performance (target question: 73.3% of hits and 2.11% of false alarms for the blue molecule, 77.4% of hits and 3.47% of false alarms for the green molecule; filler question: 59% of hits and 15.9% of false alarms for the blue molecule, 60.8% of hits and 14% of false

alarms for the green molecule, Fig. 1d). There was no difference in behavioral performance between the two molecules (all ps > .10), nor between the trials that implied different off-target conditions (see Methods and Supplementary Figure 4, 5, 6, and 7).

Egocentric-like representations of conceptual spaces in medial parietal cortex: evidence from fMRI adaptation

To examine whether conceptual goals elicited egocentric-like codes during mental search, we applied an fMRI adaptation analysis previously used to investigate brain activity during allocentric spatial and conceptual navigation [9,17]: we looked for brain regions where activation was reduced as a function of the time passed since the same egocentric-like condition (e.g., direction of 45° right to the goal) was presented (Fig. 2b). Whole-brain analysis revealed significant adaptation in the medial occipito-parietal cortex, extending along the parieto-occipital sulcus and the precuneus (peaks at $MNI_{x,y,z}$ coordinates: 6 -92 22, -12 80 48, and -4 -76 30, t = 5.83, 5.68, 5.67 respectively, Fig. 2c), similar to previous studies investigating egocentric reference frames in spatial tasks [26-29]. Smaller clusters were observed in the superior frontal gyrus, close to frontal eye fields ($MNI_{x,y,z}$: -28 28 54, t = 6.89), and in other visual and parietal regions, see Table 1. Notably, the adaptation effect in the medial occipito-parietal cortex positively correlated with participants' performance (Pearson's correlation with % of hit; r = 0.37, p = .018, see Fig. 2d), and it was present when we excluded on-target trials (Fig. 2e "off-target" and Supplementary Figure 8), when we focused on each molecule separately (Fig. 2e "blue" and "green" and Supplementary Figure 9), and when we controlled for distance from the goal (Fig. 2e "distance controlled" and Supplementary Figure 10). The effect was also present (although weaker) when we repeated the analysis only considering the left vs right position of the goal ignoring the angular distance (Fig 2e "left vs right" and Supplementary Figure 11), when we controlled for repetition of the starting point (Fig 2e "starting point controlled" and Supplementary Figure 12), or when we controlled for the signal representing allocentric "head-direction like" activity (Supplementary Figure 13).

Egocentric-like representations of conceptual spaces in medial parietal cortex: evidence from MVPA

To further validate our results, we implemented a whole-brain searchlight multivariate analysis, training a classifier to distinguish between egocentric-like angular conditions in one context (e.g., blue molecule) and testing it in the other one (e.g., green molecule, see Methods and Fig. 2e). This revealed a widespread network of brain regions consisting of the OFC/PFC ($MNI_{x,y,z}$= -36 20 -6, t = 8.29), the right IPL ($MNI_{x,y,z}$= 44 -40 54 t = 7.2), the basal ganglia (BG, $MNI_{x,y,z}$= -2 4 -4, t = 6.86), the left middle temporal gyrus (MTG, $MNI_{x,y,z}$= -54 -48 -10, t = 6.72), the left IPL ($MNI_{x,y,z}$= -54 -32 44, t = 6.47), and the posterior parietal cortex (PPC) extending to the retrosplenial cortex (RSC) ($MNI_{x,y,z}$= 4 -40 36, t = 6.24) that similarly represented egocentric-like conditions across the two contexts (Fig. 2f). For the PPC-RSC, the effect was significant also for individual contexts (p = .007 for both blue and green contexts), although weaker compared to the cross-context situation (mean accuracy = 3.93% and 3.84 above chance level for blue and green context separately, while it reached 5.49% above chance level in the cross-context analysis, see also Supplementary Figure 14). Crucially, the PPC-RSC effect remained significant also when on-target trials were removed (Supplementary Figure 15). By intersecting the whole-brain statistical maps obtained from

the two approaches (univariate adaptation and multivariate decoding, Fig. 2g), we obtained a single cluster in the precuneus, with a center of mass at $MNI_{x,y,z}$ coordinates -1, -59, 43 and an extension of 102 voxel, that was anatomically remarkably close to the brain region reported by Chadwick and colleagues [27] for the representation of egocentric goal directions (front vs left vs right vs back) during a spatial orientation task (peak at $MNI_{x,y,z}$ -6 -61 39). We used our resulting cluster to recover a low dimensional projection of how egocentric-like conditions were represented in this region using multidimensional scaling (Fig. 2h), illustrating both the distinct clusters for left vs right as well as the angular direction-specific representations.

Egocentric-like representations of conceptual spaces in behavior: evidence from eye movements

To conclusively determine the egocentric nature of these representations, we looked for a confirming signature in participants' behavior. In orientation tasks, a typical signature of spatial allocation of attention is provided by eye movements and gaze behavior. We reasoned that if participants conceived the mentally navigated conceptual spaces in egocentric terms, this might be reflected in their spontaneous eye movements. More specifically, we asked whether participants moved their eye to the right or left when the goal was to the "right" or "left" (as in, two opposite sides) in the conceptual spaces, compared to their current stimulation. Rather than being a confounding variable, this would provide conclusive evidence of the true egocentric nature of the representations we reported.

To answer our question we used the recently developed DeepMREye toolbox [35], a convolutional neural network that decodes gaze position from the magnetic resonance signal of the eyeballs. We used a set of pre-trained weights, freely available from the toolbox website and resulting from previous experiments where concurrent BOLD and eye-tracking signals were recorded [36-38], to obtain the estimates of gaze position for each fMRI volume, in each run and subject. First, we wanted to make sure that the tool could be reliably applied to our dataset. To do so, we focused on the period of the Target question, where participants had to choose between the answers "yes" and "no", which were presented on the left or right side of the screen (counterbalanced across trials). We correlated the trial-by-trial choice of the subjects (selected option on the left or option on the right) with the trial-by-trial gaze change after the question onset, under the assumption that participants are likely to look towards the chosen option. Specifically, we expected a positive correlation with gaze change on the horizontal axis and not with the vertical one, which was confirmed (mean correlation for the horizontal movements = 0.028, p = .0004).

Then, having demonstrated that a reliable left vs right information can be decoded using deepMReye, we applied the same logic to our question of interest. Specifically, we looked at eye movements indicated by the difference between the starting of the morphing period and the starting of the imagination period: by subtracting the former to the latter, we obtained a positive result if the subjects moved their eyes to the right and a negative one if they moved them to the left (Fig 2i). We then extracted, for each trial, the implied position of the goal in the conceptual space respective to the current trajectory (that is, the egocentric condition: -135°, -90°, -45°, 0°, +45°, +90°, +135°). We then correlated the trial-by-trial vector of eye movements with the trial-by-trial vector of where the goal should be in the conceptual space from an egocentric point of view. Confirming our hypothesis and the above reported results, we observed a significant positive correlation with the horizontal eye movements (mean Pearson's correlation = 0.02; p = .022) and a null correlation with the vertical eye

movements (mean Pearson's correlation = -0.005; p = .53)(Fig 2j-l). The effect was present when we focused on both contexts separately, although to a weaker extent due to the smaller number of trials, without a statistically significant difference between them (p = 0.68)(Fig 2k). Taken together these findings indicate that participants are representing the conceptual spaces using egocentric codes and perspectives.
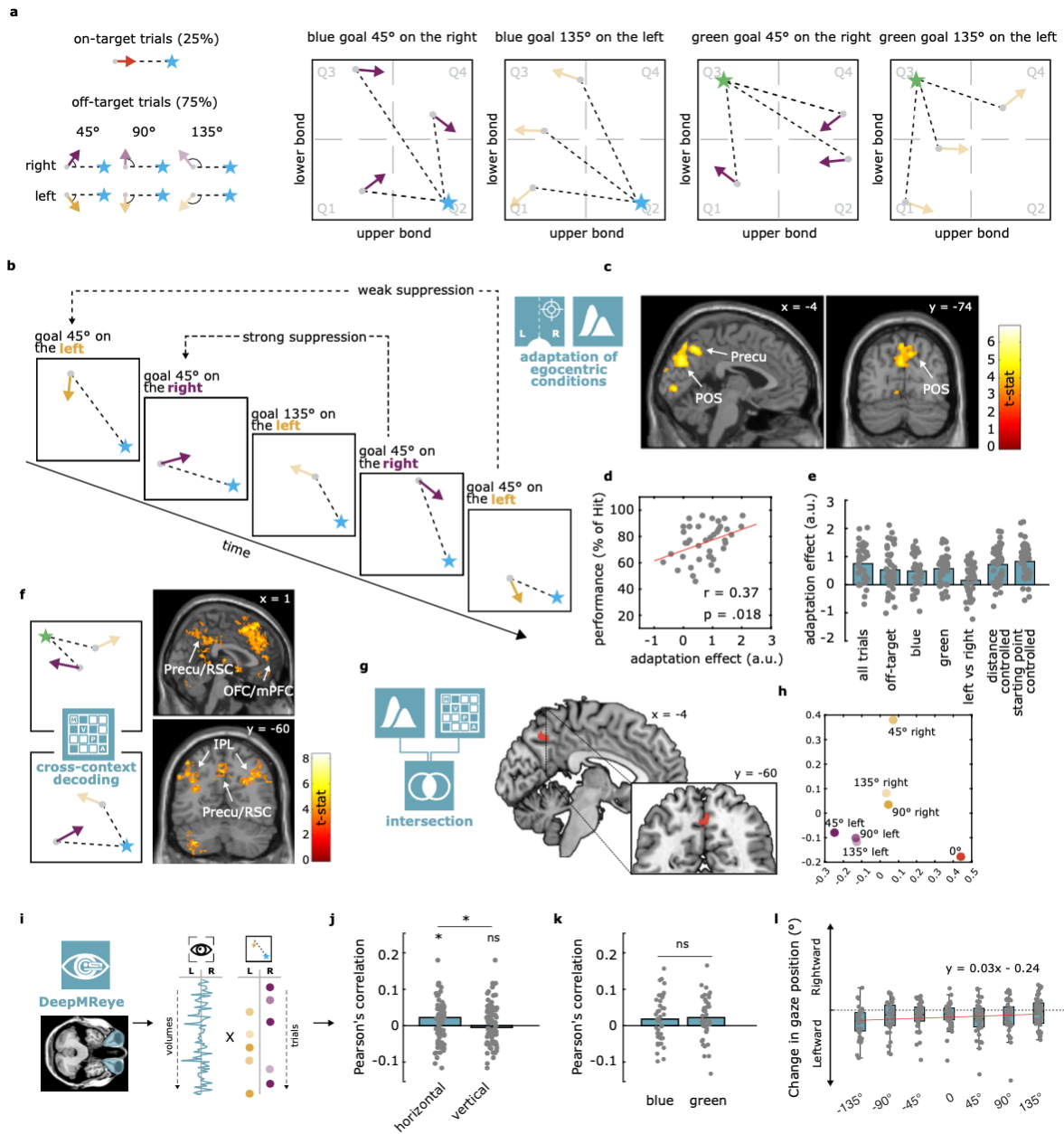
Fig. 2 | Evidence of egocentric-like coding in the medial parietal cortex. a, Morphing trajectories could happen anywhere in the environment, but they could subtend only 7 possible angular conditions to the goal ("egocentric conditions"; -135°, -90°, -45°, 0°, +45°, +90°, +135° referred to the linear trajectory from respective starting point). For instance, two trajectories could be identical in egocentric-like terms if they subtended the goal at -45°, independent of their starting position in the environment or the context they referred to (blue or green). **b**, Adaptation approach, where we modeled fMRI BOLD signal as a function of the log time passed between two presentations of the same egocentric condition. **c**, Results of the adaptation analyses, thresholded at p<0.001 at voxel level, corrected for multiple comparisons at cluster level with p<.05. **d**, Pearson's correlation between adaptation effect in the medial occipito-parietal cluster and percentage of Hit during the recall task **e**, Control analyses in occipito-parietal cluster, considering i) only "off-target" trials, ii) "blue" and iii) "green" contexts separately, iv) whether the goal was on the "left vs right" without considering the angular distance, and egocentric-like responses after controlling for vi) distance from the goal or vii) repetition of the same starting point. For all the control analyses mentioned above, Supplementary Figures from 8 to 12 report the unbiased whole-brain statistical analyses, while this panel reports participants' scores and their average in the main occipito-temporal cluster without statistics, to avoid circularity. **f**, Cross-context decoding approach, where a classifier is trained to distinguish egocentric conditions in one context and is then tested in the other one, and vice versa (see Methods). Results are thresholded at p<.001 at voxel level, corrected for multiple comparisons at cluster level with p<.05. **g**, Anatomical intersection between the brain maps resulting from the adaptation analysis and the cross-context decoding. **h**, Multidimensional scaling of the egocentric conditions. Patterns of activity are extracted from the cluster in precuneus (peak from intersection analysis). **i**, We used the DeepMReye toolbox (Frey, Nau & Doeller 2022) to extract gaze behavior starting from the BOLD signal from the eyeballs. For each trial, we extracted the eye movements when participants were processing goal position in conceptual space compared to their current stimulation/trajectory, and we correlated with the "true" position of the goal in conceptual space. **j**, Fisher-transformed Pearson's correlation score was significant at group level for horizontal eye movements, not for vertical. **k**, the effect was present in both contexts, although to a weaker extent, without differences between the two. **l**, regression line showing the linear relationship between egocentric angles of goal position in conceptual space and leftwards vs rightwards eye movements. * p < .05; ns = not significantly different

Evidence of mental rotation of conceptual spaces in parietal cortex

Egocentric perspective during goal-directed spatial orientation has been linked to the ability of transforming and rotating existing memory representations of our surroundings, enabling the retrieval of experienced viewpoints to the goal and correct heading directions [39,20]. A candidate faculty supporting this mechanism is mental rotation [40], namely the ability to rotate the representations of objects or scenes held in mind to match their visual appearances. Both neuroimaging and non-invasive brain stimulation indeed indicate that the crucial cortical nodes supporting mental rotation in the human brain are located in the parietal cortex [41,42], consistent with the proposal of a dedicated neuronal population in this region, referred to as "parietal window" [21], that is recruited for egocentric transformations during mental exploration and spatial orientation. We reasoned that a similar mechanism could also operate during goal-directed navigation in conceptual spaces, when we need to ignore or adapt their allocentric map-like representations to favor egocentric reference frames, more centered on the relation between goals and our current state. Therefore, we hypothesized that the representation of the two contexts mentally navigated by the participants in our experiment might be rotated in such a way that it would match the location of the current goal, thus equating the focus of their parietal window. To test this, we extracted activity patterns for the 4 quadrants separately for the two contexts and we looked, using a whole-brain searchlight, for brain regions that had an increased similarity between the quadrants in one context (e.g., blue molecule) with the corresponding quadrants in the other one (e.g. green molecule) after the feature space was rotated by 180° to align the goal locations in both contexts (e.g., the activity evoked by trials occurring in quadrant 1 (Q1) for the blue molecule would be more similar to that evoked by trials in Q4 for the green molecule, see Methods and Fig. 3a). The results revealed significant clusters in the precuneus ($MNI_{x,y,z}$= -2 -56 46, t = 4.5) and in the bilateral IPL (left: $MNI_{x,y,z}$= -32 -62 40 t = 4.93; right: $MNI_{x,y,z}$= 36 -56 42, t = 4.89, see Fig. 3b), that comprise the brain regions previously reported to be involved in mental rotation of visually displayed objects [41,42] as well as egocentric processing [27,28]. This effect could not be explained as a simpler cross-context correspondence of goal-quadrants (vs non-goal quadrants) because it was still present when we removed them from the analysis (Fig. 3c middle panel and Supplementary Figure 14), nor as cross-context similarity of distance from the goal, because in the precuneus it remained significant (although to a weaker extent) also when we only considered Q1 and Q4, that were at the same distance from the goal (Fig. 3c right panel). This finding suggests that the parietal representation of conceptual spaces is transformed and re-oriented to maintain the focus on goals and their relation with our current state, independently of the global map.
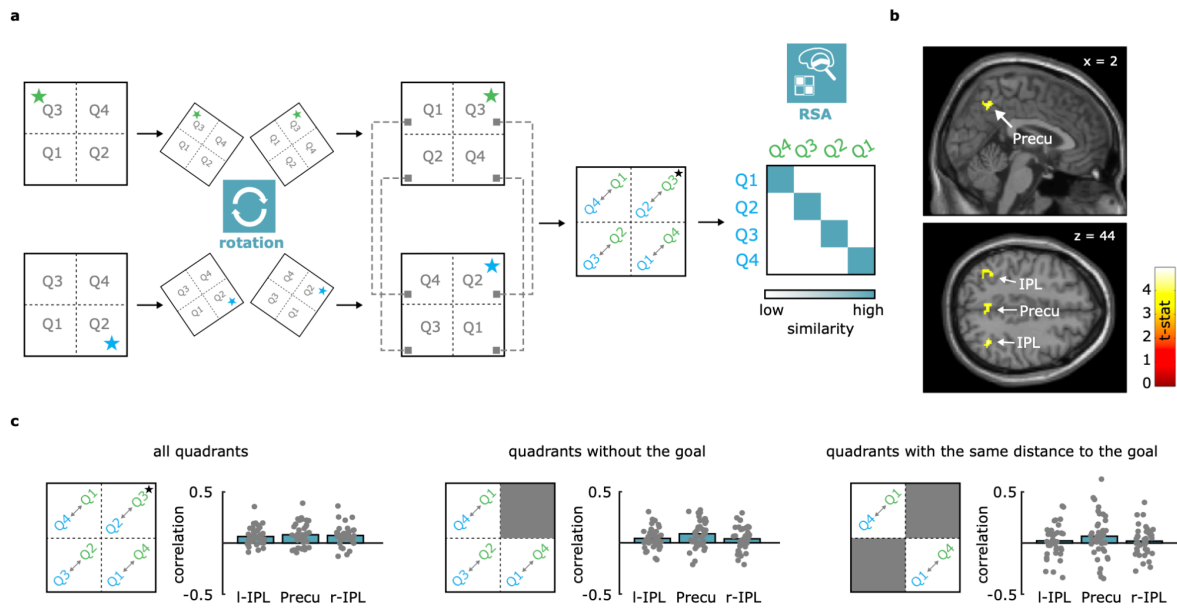
Fig. 3 | Evidence for a goal-directed mental rotation of the feature maps in the parietal cortex. a, Logic of the rotation analysis, where quadrant-by-quadrant similarity was measured after assuming a rotation of one of the two spaces (see Methods). On the right, whole-brain results of the correlation analysis, thresholded at p<0.001 at voxel level, corrected for multiple comparisons at cluster level with p<.05. **c**, Control analyses confirm the effect is not driven by goal quadrants alone (middle panel and Supplementary Figure 16), and that this is not, at least in the precuneus, a mere effect of distance from the goal (right panel). Please note that for this last control analysis, no effect was detected at an unbiased whole-brain level, not even at a threshold of p<.05, probably because of the low number of remaining trials, as the same happened when we considered other pairs of quadrants only.

Evidence for goal-induced alteration of grid-like representations in entorhinal cortex, medial prefrontal cortex and superior parietal lobule

During spatial navigation, egocentric representations are complemented by a parallel reference frame, reflected in allocentric map-like models of the navigated environment [5]. Such "cognitive maps" in mammals depend mostly on the activity of the hippocampal-entorhinal circuit. A key neural signature of an allocentric map are entorhinal grid cells [8]. In fMRI, a proxy measure of grid cell population activity can be observed: the fMRI signal is systematically modulated as a function of movement direction (hexadirectional activity [9]), where trajectories that are at multiple of 60° apart from each other ("aligned") are represented more similarly than those that are not ("misaligned")[39]. Thus, to investigate the effects of conceptual goals on allocentric cognitive maps, we first looked for signatures of the grid-like code. We implemented a variation of the grid-RSA approach previously employed by our groups [43,17] and others [14]: for each trajectory in one context (e.g., green molecule), we assumed higher pattern similarity in the entorhinal cortex for those trajectories in the other context (e.g., blue molecule) that were aligned to multiple of 60°, and lower pattern similarity for those that were misaligned (see Fig. 4b for the predicted model. Note that the egocentric mental rotation reported above would not affect this analysis, since a rotation of 180° is a multiple of 60°). We found that i) the similarity was higher for aligned compared to misaligned trajectories in the left posterior-medial entorhinal cortex (left pmEC, mean Pearson's r = 0.03, std = 0.10, p = .01; right pmEC: mean Pearson's r = 0.02, std = 0.10, p = .09, Fig. 4c), ii) that this effect was not present in the anterolateral entorhinal cortices (all p > .91), and iii) that control periodicities did not elicit the same effect (all p>.09, Fig. 4d). We found the 6-fold modulation in the left entorhinal cortex also using a whole-brain searchlight procedure ($MNI_{x,y,z}$= -12 -14 -28, t = 3.36, p<.005 at voxel level, uncorr., Fig. 4e). Thus, we observed a signature of allocentric maps, namely grid-like representations in the entorhinal cortex, during our conceptual task, concurrently with the egocentric-like signatures in the parietal lobe, as predicted in ref [6]. Interestingly, recent evidence suggests that goal locations alter rodents' grid-like map during spatial exploration [33,34]. We reasoned that this mechanism, if paralleled during conceptual search, might support the readout and access of conceptual goals, as it would potentially differentiate behaviourally relevant regions of conceptual spaces to irrelevant ones. Therefore, we asked whether the grid-like code is modulated as a function of distance to conceptual goals. To examine this question, we used a different approach, partially inspired by Doeller and colleagues (2010), that allowed us to conduct a more fine-grained quadrant-specific grid analysis as a function of goal proximity. More specifically, we followed a repetition suppression approach where each trajectory was assumed to evoke a signal that scales as a function of the angular distance in 60° rotational space compared to the previous one. For instance, a trajectory at 90° would elicit a weak (suppressed) signal if presented after one at 30° because they would be 60° apart, thus perfectly aligned in the 6-fold rotational space, while the same trajectory would elicit a stronger signal if preceded by one at 0° because they would be 30° apart in the 6-fold rotational space. Following our hypothesis, we modeled the grid-like modulation separately for the four quadrants, where trajectories were evenly sampled and distributed (see Methods). Among these four quadrants, one contained the goal, and was considered as at a "close distance" from it (e.g., Q2 in blue context), two were at the same "medium distance" from the goal (e.g., Q1 and Q4 in blue context, and were thus averaged) and one was at a "far distance" from the goal (e.g., Q3 in blue context). If allocentric grid-like maps are involved in representing goal locations during conceptual navigation, we expect the grid-like

signal to be modulated as a function of the quadrant, that is, as a function of the distance from the goal. More specifically, given the above-mentioned empirical evidence in rodents of increased grid-cell activity around goal locations (both in terms of firing rate and number of grid fields), we expected these putative regions to show a weaker grid-like signal for trajectories happening in quadrants far from the goal (Q3 in the blue context, Q2 in the green context), a medium grid-like signal for those happening in quadrants at medium distance from the goal (Q1 and Q4, identical for the two contexts), and a stronger grid-like signal for the trajectories in goal quadrants (Q2 in the blue context, Q3 in the green context) (see Methods and Fig. 4f). A whole-brain analysis revealed this modulation in regions where grid-like signals have been previously observed for navigation in both virtual reality and conceptual spaces [12,15]: the right entorhinal cortex ($MNI_{x,y,z}$= 16 -6 -26, t = 4.23, p<.001, small volume corrected with bilateral EC mask), the medial prefrontal cortex (mPFC; $MNI_{x,y,z}$= 2 48 -2, t = 4.46, p<.001 corrected for multiple comparisons at cluster level with p<.05), and the superior parietal lobule (SPL; $MNI_{x,y,z}$= -30 -46 66, t = 5.18, p<.001 corrected for multiple comparisons at cluster level with p<.05; Fig. 4g): here, the grid-like signal changed as a function of goal proximity, being relatively weaker for trajectories that were far apart from goal locations and stronger close to the goal, see Fig. 4h. An additional, weaker cluster was observed in the left angular gyrus, see Table 3. Taken together, these results indicate that a typical signature of the cognitive map, the grid-like code, is modulated by the presence of conceptual goals.
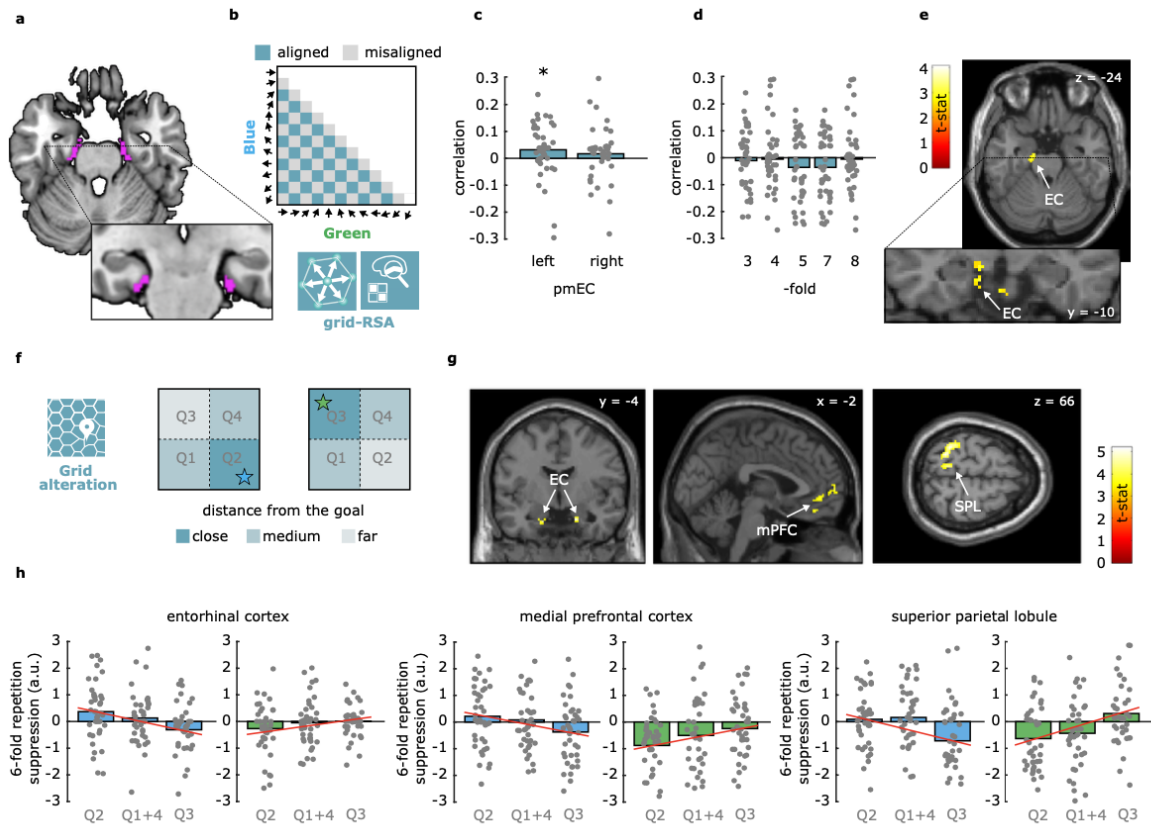
Fig. 4 | Evidence of grid-like coding in left pmEC and of its alteration in right pmEC, mPFC, and SPL. a, ROIs of posteromedial entorhinal cortex (pmEC) taken from ref. [64]. **b**, Logic of the cross-context grid-RSA, where patterns of activity evoked from morphing trajectories in one context are correlated with those in the other one assuming a 60° rotational similarity (e.g., moving at 30° in the blue context would be more similar to 90° in the green context than 0°). The model matrix shows aligned and misaligned pairs, for which we predicted higher and lower similarity, respectively. The diagonal is excluded to avoid biased effects of homologous directions across the two contexts. **c**, a significant (p<0.02) grid-like effect is observed only in the left pmEC. **d**, None of the control symmetries showed significant effect in the left pmEC. **e**, Whole-brain results of the same effect, here shown thresholded at p<0.01 uncorr. for visualization purposes. **f**, Logic of the goal-related analysis, where we expected difference in the grid-like code as a function of quadrant, that is, as a function of goal distance. **g**, Whole-brain results thresholded at p<0.001 at voxel level, corrected for multiple comparisons at cluster level with p<.05 (EC small volume corrected with bilateral pmEC mask shown in panel a). **h**, visualization of the linear effect across quadrants and contexts, indicating that the alteration followed goal position across the two spaces, blue and green. Q1 and Q4 are averaged, as they are equidistant from the goal. Please notice that averaging before running individual subject-level glm or after that did not affect the results.

Discussion

Learning how the human brain supports the access to stored conceptual information is of critical importance for understanding our cognitive abilities. A fascinating hypothesis put forward in recent years is that a phylogenetic continuity exists between the brain spatial navigation circuits and the human conceptual system, with concepts memorized as points of internal cognitive or conceptual maps in the medial temporal lobe [18,3]. The discovery that humans can recruit the hippocampal formation to represent how concepts in memory relate to each other supports this proposal [12-17], but the human spatial navigation system comprises an extended network of brain regions beyond the medial temporal lobe, that represents space via complementary allocentric and egocentric frames of reference [20-22]. Recently, we have hypothesized that this fully integrated network might support conceptual "navigation" across these different reference frames, for instance guiding us during mental search [6]. In support to this hypothesis, we here reported three main novel findings, showing that during mental search conceptual goals are tracked in parallel across different reference frames. First, we showed evidence of egocentric-like codes in the parietal cortex to represent goal position in conceptual spaces relative to our current state or experience. This was confirmed by an additional analysis of eye-movements: participants were moving their eyes to the left or to the right consistently with the position of the goals in conceptual space, thus revealing that they were mentally searching for concepts using a first-person, self-centered, perspective. Second, we showed that the representation of the two conceptual spaces in the parietal cortex were rotated to match goal positions across contexts. Finally, we showed that the brain supports mental search in conceptual spaces by concurrently altering the structure of the allocentric grid-like code in medial temporal, prefrontal, and superior parietal cortices as a function of goal proximity. Taken together, these representational schemes might provide the critical information of "where" goals are stored in conceptual spaces, employing both egocentric and allocentric reference frames in parallel.

According to an influential model of spatial memory and imagery [20-22], the parietal cortex and the medial temporal lobe are the two major hubs of our spatial navigation system, providing a representation of the external navigable space across different reference frames. In this perspective, the parietal cortex holds egocentric codes that capture the locations of objects and landmarks in self-centered coordinates (e.g., whether an object is to our left or to our right), as demonstrated by several empirical findings [23-31], see Introduction. In our study, we reported remarkably similar observations in the parieto-occipital sulcus (POS), the precuneus, and the PPC extending to the RSC. These regions represented goal locations in conceptual spaces according to a reference frame that was independent from the position of the goal across contexts, the allocentric angle of the trajectory, and the current allocentric position in space. This representational scheme can be interpreted as an egocentric vector relative to the goal: Akin to the physical world, where we can tell whether an object is to our left or right while we move and change position in the environment, here, by considering how the aspect ratio of the molecule stimuli changed, we could define to what degree a goal concept was on one side or the other in the underlying feature space, irrespective to its external geometry. This indicates the recruitment of egocentric-like schemes in the parietal cortex for representing conceptual goals. The role of the parietal cortex beyond spatial cognition has been previously reported in studies on conceptual/semantic access and on autobiographical memory (see reff. [44-45,53]). They have suggested the precuneus and the

inferior parietal lobules as key regions of these networks. However, a direct link between the representational codes typically evoked in this region during spatial navigation and more abstract conceptual processing has been formulated only recently, with fMRI studies revealing similar parietal activity when participants have to evaluate the spatial proximity of locations, the "temporal proximity" of events and the "emotional proximity" or people, from an egocentric point of view (namely, how far/close from one's own self; see reff. [46-50]. The present results go beyond these previous reports by revealing egocentric vector coding as a function of goal location during conceptual navigation. In full support of this position, the additional evidence coming from the analysis of eye movements using DeepMReye confirmed that participants were employing a first-person perspective of the conceptual spaces while mentally searching through them. In sum, our findings support the idea humans represent goals in conceptual spaces using an egocentric reference frames, relative to our specific self-centered perspective and experience, beyond the spatial domain, as theoretically predicted in our recent account on the cooperation between parietal and medial temporal regions in conceptual knowledge representation across reference frames [6].

This account also stresses that, besides egocentric representations in the parietal cortex, physical environments are also represented in our brain using a complementary coding scheme tuned to an allocentric perspective, namely viewpoint-independent representations of the general layout of the environment [20-21]. A typical signature of allocentric representations in the brain is the grid-like code, likely originating from the population activity of grid cells, and typically observed in the medial entorhinal and prefrontal cortices in humans engaged in both virtual and conceptual navigation [9]. Interestingly, two recent studies reported that entorhinal grid cells in rats change their firing pattern in the proximity of goals, where an increased number of firing fields as well as a reduced distance between them was observed [33,34]. Whether this also applies to human grid-like representations during spatial navigation is still unclear, especially given the difficulty to draw direct comparisons between individual neural activity patterns in rodents and indirect neuroimaging measures in humans (but see [55]). Nevertheless, we reasoned that such a mechanism would be, in principle, extremely useful for the readout of conceptual goals from cognitive maps, as it would provide an allocentric signature of goal positions in conceptual spaces that is complementary to parietal egocentric-like codes. By implementing a novel grid-like analysis as a function of distance from the goal, we indeed showed that the grid-like signal in the right entorhinal cortex, in the medial prefrontal cortex, and in the superior parietal lobule was weaker for regions of the conceptual environments that were not behaviourally relevant, while it was relatively stronger for regions containing a goal. This indicates that the grid-like code might not provide a mere metric of space, physical or conceptual, that reflects the general layout of the navigable environment, but it might also be recruited for the representation of task-relevant conceptual regions [19], such as specific goal concepts.

Whether and how this is related to goal-directed, egocentric-like responses in the parietal cortex remains unclear. According to models of spatial navigation and memory [21,22,49], allocentric representations in the hippocampal-entorhinal system interact with the egocentric ones in the parietal lobe via the medial parietal cortex and, in particular, the retrosplenial complex (RSC), with information flowing in one direction or the other on the basis of task demands. For example, when we mentally construct the general allocentric layout of a visited environment from different perspectives, the information is supposed to be directed from parietal to medial-temporal cortices; on the contrary, when we recover from memory a specific image or scene of an episode, the information would flow from the medial-temporal lobe to the parietal cortex. In both cases, the RSC is thought to provide a transformation of

the reference frame (from egocentric to allocentric, or vice versa). Although we did observe activation in the PPC/RSC in our decoding analysis, the exact role of this region and whether it was involved in transforming one reference frame into the other during our conceptual navigation task could not be determined. It is possible that the alteration of the grid-like map is beneficial for orienting the focus of our "parietal window" (correspondent to the observer in spatial navigation tasks, according to models of spatial memory [21]) towards the goal, thus resembling the hypothesized top-down effect proposed for reconstructing specific egocentric scenes from allocentric maps [21]. This would be in line with recent evidence that perturbing the grid-like code in rodent entorhinal cortex impairs egocentric-like representations in the RSC [50], but whether this also applies to the access to conceptual knowledge, or the underlying computational principles that allow the brain to operate this transformation, is unknown. Future studies could address the interplay between the parietal cortex and the medial temporal lobe during conceptual search by investigating, for instance, the connectivity profile between the two regions as a function of the task at hand.

Finally, in our study we also reported an intriguing additional observation, namely the rotation of the representation of the two contexts in both the medial and the lateral parietal cortices: in these regions, the representations of the two contexts were highly similar when they were rotated in such a way that goal positions (or quadrants, in our case) were perfectly aligned. This effect is reminiscent of the well-known phenomenon of mental rotation, which is dependent on the parietal cortex, as demonstrated by both neuroimaging and non-invasive brain stimulation [40-42], and has been proposed as a candidate mechanism for viewpoint-dependent orientation [39]. Thus, one interpretation of this finding is that conceptual spaces might be rotated in the parietal cortex to maintain the center of the "parietal window" on the task-relevant conceptual goals, and that this might be a crucial stage in the process of orienting and transforming egocentric representations into allocentric ones [20-22]. At the present stage, this interpretation remains speculative and further investigations are needed to provide empirical support to this hypothesis. Yet it also generates further intriguing speculations on the role of mental rotation abilities as a precursor of more abstract and sophisticated forms of "conceptual rotation", for instance in social settings, where we need to change "our perspective" to better understand others' positions and mental states.

To conclude, we reported evidence that conceptual goals are encoded via egocentric-like representations in the parietal cortex and that they alter the allocentric grid-like map in the medial temporal and prefrontal cortices. These results can contribute to our understanding of how humans organize and search for conceptual information in memory, and support the proposal that, in our species, the brain's navigation system can be repurposed to represent knowledge across different reference frames [6].

Methods

Participants

Participants were 40 adults (19 females) with mean age = 27.2 years (std = 4.8). They all gave informed consent and were reimbursed for their time with 9 euros/hour for behavioral tasks and 10 euros/hour for the fMRI scanning session. All had normal or corrected-to-normal vision, no history of neurological diseases, and were right-handed. Sample size was determined without an priori power analysis, due to the small number of experiments conducted in conceptual navigation and no existing research testing specifically the egocentric code in concept spaces. Moreover, the study involved several different types of analysis (fMRI adaptation, multivariate decoding, grid-like analyses), in addition to behavioral analyses, which further complicated the determination of an effect size of reference in previous literature. In an attempt to decide the relatively appropriate sample size, we took guidance from studies in this area which have drawn informative results from smaller pools of participants. For example, in studying goal direction signals in a spatial task, Chadwick and colleagues (2015) included 16 adult participants. In a study that was very influential in the development of our own (but that focused on allocentric coding schemes), 21 participants performed similar tasks [12]. Based on these considerations, we refrained from forming precisely quantified expectations and aimed to test 40 participants, which was roughly twice the number tested in the majority of experiments in this area that consistently showed similar results for allocentric and egocentric navigation. The study did not include between-group analyses, thus no blind assignment was performed. The study was approved by the local Ethics Committee of Leipzig University, Germany (protocol number 159/21-ek).

General experimental design and cover story

The experiment consisted of 3 days. At the beginning of the first day, after signing the informed consent, participants were told the cover story of the experiment: they were asked to play the role of scientists in a future society where mankind lives in peace and prosperity thanks to the development of two molecules, called Megamind and Megabody, able to enhance cognitive and physical abilities, respectively. Molecules were fictitious and just represented visual stimuli on the computer screen during the entire experiment: participants did not interact with real biological molecules or chemicals of any sort. They were told that, for the next 3 days, their task would be to learn how to produce these molecules by manipulating, through a computer program, specific reactions, in order to respond to the supply demand of the society.

During the first 2 days, participants performed a computer-based behavioral training in a laboratory setting, using a monitor pc, in order to familiarize with the feature spaces and the conceptual goals in them. During these two days, they performed three different tasks, named "Collect task with hint", "Collect task without hint", and "Recall task" (see below). Day 1 lasted roughly 1h and 30 minutes, day 2 lasted ~ 1h, as participants were already familiar with the tasks and procedures and performed faster and better (see Results in the main text). On the third and last day of the experiment, participants performed the Recall task while their brain activity was monitored using fMRI. This last procedure lasted about 2 hours.

Stimuli

We created two visual stimuli that we called "molecules" on Microsoft PowerPoint (Microsoft Corp.). These so-called molecules are just hypothetical toy examples detached from real world chemistry. Our stimuli had a central body and two extreme parts that were connected to it by two bonds, an upper and a lower one. Throughout the experiment, different molecules could vary in their "aspect ratio", namely the relative length of one bond to the other. Crucially, by considering the length of the two bonds as axes of a two-dimensional space, we could conceive each configuration (that is, a molecule with a specific aspect ratio) as a point in the two-dimensional space. Molecules were created in two colors: blue and green, which indicated the two different contexts. Participants learned that the molecule named "Megamind" was a specific configuration of the blue molecule, with a longer upper bond and a shorter lower one, and that the molecule named "Megabody" was a specific configuration of the green molecule, with a shorter upper bond and a longer lower bond (Fig. 1a). Blue molecules with aspect ratio different from the one of Megamind and green molecules with aspect ratio different from the one of Megabody were considered "wrong configurations" and did not have any behavioral relevance in the experiment (this also applies to the blue molecules with the same aspect ratio of Megabody and the green molecules with the same aspect ratio of Megamind).

Collect task with hint (behavioral training)

This task was administered at the beginning of both training days. Participants were prompted with a screen showing several elements. In the central part, they were presented with a colored molecule in a given random configuration. On the right, they had a symbol which we referred to as the "hint": this symbol was gray when the molecule shown on the screen was in the wrong configuration, and it turned blue or green when the molecule was correctly morphed in the goal configuration. On the left, they were presented with a controller composed of two vertical graded bars. Participants were told that the physical attributes of the molecule (the aspect ratio) could be changed by manipulating the amount of oxygen and hydrogen in the surrounding of the molecule: increasing the oxygen or the hydrogen would make the upper or lower bond, respectively, longer; decreasing them would make them shorter. The reference to hydrogen and oxygen was part of the cover story and they were not really manipulated in the experimental room. Participants were instructed to press the "Z" key on the keyboard to adjust the ratio of change they wanted to apply to the molecule: by doing so, the computer displayed a different relative amount of oxygen and hydrogen on the controller. In spatial terms, this was conceivable as setting a facing direction of movement. Holding the "Z" key, for instance, would continuously reset the ratio between hydrogen and oxygen, and would correspond to continuously rotating the facing direction in 360°. In other words, the hydrogen and oxygen corresponded to the sin and cosine projections of the "facing direction" vector once considered on a trigonometric circle.

Then, when the choice was made and the participant felt confident, they could apply the change to the configuration that was presented on the screen at that specific moment, by pressing "C" or "V". Holding these keys would allow the morphing/movement to continue along the same trajectory ("C") or in the opposite direction ("V"). Two horizontal bars, placed above and below the molecule at fixed distances from the central body, indicated the limits for the configurations: the two bonds could not be elongated beyond these points. Similarly, they could not be set shorter than the position of the central body. In spatial terms, these represented the boundaries of the two-dimensional spaces that were implicitly navigated. Participants were instructed to try different combinations of oxygen/hydrogen ratios to find

the correct morphing trajectory that could lead, when applied, to the goal configuration. When the morphing molecule corresponded to the correct configuration, the hint symbol turned blue or green and participants could collect the molecule by pressing the spacebar on the keyboard. In this task, this key was disabled for wrong configurations, meaning that participants could not collect wrong molecules. Subjects had 30 minutes maximum to collect 20 Megamind and 20 Megabody, with blue and green molecules presented pseudo-randomly trial after trial. A small counter placed below the hint symbol informed them on how many molecules out of 40 they had collected so far.

Collect task without hint (behavioral training)

This represented the second task participants performed on both training days. The visual appearances as well as the general demand were identical to the previous one, except for a few pivotal differences. First, the hint symbol was removed: participants had to recall the correct aspect ratio of the molecules. Second, they could collect wrong molecules, which counted as errors. Third, they performed this task separately for the blue and green molecules. Fourth, and last, they were instructed to collect as many goal molecules of a given color as possible in 3 minutes. The order of the two contexts was counterbalanced across the two days.

Recall task (behavioral training and fMRI)

This was the last task on both training days. Participants were told that they had to evaluate some of the reactions they had tried in the previous tasks in order to classify them as efficient or not to produce the goal molecules. Reactions were instead new, and created to satisfy the specific requirements of our design (e.g., balance between directions, quadrants, and so on). They performed two runs, 1 with blue molecules, 1 with green ones. For each trial, a molecule in a random configuration was shown at the center of the screen, without any other detail except for the upper and lower horizontal boundary lines. The molecule remained on the screen for 0.5 seconds, then it started morphing automatically for about 1 second, before stopping again and remaining on the screen with the updated configuration. At this point, the "imagination period" started: participants were instructed to imagine the morphing to continue in the same way, following the same changes in the aspect ratio, and to decide whether such a morphing wouldever result in the molecule matching the correct goal configuration of Megamind (for blue molecules) or Megabody (for green molecules). In spatial terms, this was conceivable as imagining the movement to continue along the same trajectory and deciding whether the goal location would be reached or missed. After 4 seconds of imagination, participants were prompted with a question asking whether they would ever obtain the correct configuration if the molecule continued to morph in the same way, and they could select one of two answers (Yes or No, with their left and right assignment on the screen balanced across trials). After the answer was given, the following trial started. This "target question" happened on a pseudo-randomly selected 50% of trials. In the remaining half, we introduced a "filler question" where, at the moment when the question was shown, we displayed a random molecule on the screen that could be "on the trajectory" or not, and we asked whether they would ever obtain *that particular* molecule if the morphing continued in the very same way (Fig. 2c). This question was introduced to induce participants to create a global map of the navigable spaces while holding in mind the conceptual goals, so that we could test concurrent representation of allocentric cognitive

maps in the brain: given that i) participants did not know in advance the kind of question they were going to be asked, and ii) that we analyzed the imagination period preceding the question (see below), we ensured the optimization of chances to detect all of our effects of interest. Participants performed the recall task also during the fMRI scanning session. The procedure remained identical, except for the fact that there were 8 runs (4 with blue molecules, 4 with green molecules, intermixed).

There were 48 trials per run, divided in the following way. Irrespective of the question asked, morphing trajectories were directed to the goal (Megamind or Megabody, catch trials) 25% of the time (12/48 trials). The remaining 75% of trials (36/48) was equally divided into 6 egocentric-like conditions, missing the goal with angular distances to the correct trajectory of -135°, -90°, -45°, +45°, +90°, +135°. The sign (+ or -, arbitrarily defined) of these angular trajectories determined whether the goal was missed on the "left" or on the "right". As the target question happened on 50% of the trials, participants were expected to answer Yes to this question on 6 trials, and No on 18, for a total of 24 trials (24/48 = 50%). In the remaining trials, when the filler question was asked, we generated molecules for the question period that could lie on the current trajectory (34% of the time), or not (33% of the time it was out of trajectory by -60°, the other 33% of the time it was out of trajectory by +60°). Given the complex and noncorresponding percentage of trials and expected responses, performance for this task was expressed as probability of Hits (probability of saying Yes when Yes was the correct answer) and False alarms (probability of saying Yes when No was the correct answer). Trials and egocentric-like conditions were also equally divided into the 4 quadrants composing the feature space, by controlling considering the midlines of both axes as boundaries. No morphing period implied a crossing of between-quadrant boundaries.

fMRI data acquisition

fMRI data were acquired at the Max Planck Institute for Human Cognitive and Brain Sciences (Leipzig, Germany) using a 3-Tesla Siemens Skyra scanner equipped with a 32-channel head coil. High-resolution T1-weighted images for anatomical localization were acquired at the end of the scan session using a three-dimensional pulse sequence with TR = 3.15 ms; TE = 1.37; flip angle = 8; voxel size = 1.6 × 1.6 × 1.6 mm). T2*-weighted images sensitive to blood oxygenation level-dependent (BOLD) contrasts were acquired using a pulse sequence with TR = 1500 ms; TE = 22 ms; flip angle = 80°; voxel size = 2.5 x 2.5 x 2.5 mm; multiband acceleration factor of 3. Participants viewed the stimuli on the screen through a mirror attached to the head coil, and behavioral responses were collected using a button box.

Preprocessing

Images were preprocessed using a standard pipeline with SPM12, which included slice-time correction, realignment of functional images to the middle scan of each run, coregistration of functional and anatomical images, segmentation, normalization to the Montreal Neurological Institute (MNI) space, and smoothing of 5 mm isotropic.

Egocentric-like adaptation analysis

We defined a first-level generalized linear model (GLM) for each participant by modeling, in one regressor, the onset of the imagination period for each trial, modeling trial duration for

the entire imagination period. Following previous studies [9,17], we applied a parametric modulator to this regressor where we included, for each trial, the (log) time passed since the last presentation of the same egocentric-like condition (e.g., since the last time that a trajectory with the goal at -45° was presented)(Fig. 3b). Trials with the first presentation of a given egocentric condition were excluded. Additional regressors of no interest (included also in all the subsequent analyses) modeled the time of response (1 regressor) as well as movement parameters (6 regressors). Group-level (2nd level) analyses were conducted using SPM12 by running voxel-by-voxel t-tests of these contrasts across subjects. Corresponding analyses were performed when controlling for additional factors, such as removing catch trials (all the egocentric-like conditions directed to the goal), separating runs for blue and green molecules, or modeling left vs right (see main text for the full list).

Cross-context decoding of egocentric-like conditions

We ran a second GLM, modeling each egocentric-like condition separately (trajectories with a direction -135°, -90°,-45°,0°,+45°,+90°,+135° to the goal). We then used the MATLAB (Mathworks Inc.) toolbox COSMoMVPa [51] to run a searchlight cross-context decoding approach. We defined spheres of radius of 3 voxels (consistent with previous studies (e.g., 16) centered on each voxel of the brain and, within these regions, we extracted the activity pattern for each egocentric-like condition, separately for the two molecules. We used a Nearest-Neighbor (NN) classifier as implemented in the COSMoMVPa toolbox to distinguish the 7 egocentric-like conditions in one context (e.g., blue or green) after training it on the activity patterns evoked in the other context (e.g., green or blue), using a cross validation scheme. From the accuracy level we subtracted the chance level (1/7 = 14.29%) and we stored the resulting performance of the classifier at the center voxel of each sphere, creating one brain map per subject. Group-level analysis was performed with SPM12. Corresponding analyses were performed by excluding catch trials (egocentric-like conditions of 0°) and considering a chance level of 1/6. Corresponding results were obtained using a Linear Discriminant Analysis (LDA) classifier as implemented in the COSMoMVPa toolbox.

Rotation of the feature spaces

We ran a GLM with 4 regressors of interest, each one modeling trials that were happening in one of the 4 quadrants of the conceptual space, separately for the two molecules (Q1 blue, Q1 green, Q2 blue, Q2 green, and so on). We used COSMoMVPa to run a whole brain searchlight (spheres with radius 3 voxels) using a cross-context correlational approach. We constructed a similarity matrix where the activity patterns separately evoked by the four quadrants in one context (Q1 blue, Q2 blue, Q3 blue, Q4 blue) were correlated (Pearson's r) with those in the other one in reversed order, as if the space was rotated 180° (Q4 green, Q3 green, Q2 green, Q1 green). We looked for brain regions where correlation values on diagonal (representing the correlations Q1 blue → Q4 green; Q2 blue → Q3 green, Q3 blue → Q2 green, Q4 blue → Q1 green) were higher than off-diagonal, storing the Fisher's-to-z transformed on- vs off-diagonal difference in the center voxel of each sphere and creating one map per subject, that were later analyzed at the group-level using SPM12.

Cross-context grid-RSA

To investigate the presence of a grid-like signal during goal-directed conceptual navigation, we implemented a variation of the grid-RSA [16,14,43]. We first resampled all the allocentric movement trajectories in bins of 30° with the direction 0° arbitrary aligned to the horizontal axis. We run a GLM modeling the resulting 12 conditions (0°, 30°, 60°, 90°, 120°, 150°, 180°, 210°, 240°, 270°, 300°, 330°) separately for the two contexts, and we then moved to multivariate analyses within the COSMoMVPa environment. We constructed a cross-molecule similarity matrix, where the activity patterns of each of the 12 allocentric directions from one context were correlated (Pearson's r) with those from the other context. The resulting matrix was made symmetrical by averaging the lower and upper triangle, and the diagonal was removed, to ensure that any potential grid-like effect was not driven by higher similarity between homologous directions across the two environments. We constructed a predicted model which assumed, for each movement direction in one context, higher similarity with those movement directions in the other context that were at multiples of 60° from it (Fig. 4b). For example, moving at 30° in the blue context would elicit higher similarity with movement directions of 90°, 150°, 210°, 270°, and 330° in the green context, that were referred to as "aligned" ,compared to the remaining ones ("misaligned"). We thus correlated (Pearson's r) the lower triangle of the neural similarity matrix with the lower triangle of the model, and stored the Fisher's-transformed correlation values for each subject. We applied this analysis at first in a Region of Interest in the postero-medial entorhinal cortex, and in control regions in the antero-lateral entorhinal cortex, using masks from ref. *(52)*. We then applied the same analysis in a whole-brain searchlight, using spheres with radius of 3 voxels. Control models were developed in the same way but assuming rotational symmetries of 120° (3-fold), 90° (4-fold), 72° (5-fold), 51.4° (7-fold), and 45° (8-fold).

Alteration of the grid-like code

To investigate the possibility of an alteration of the grid-like code, we proceeded using a repetition suppression approach, that allowed us to analyze the grid-like code as a function of goal proximity. Our trials were equally divided into 4 quadrants: one of them contained the goal, two were at a medium distance from it, and the last one was far from the goal. Importantly, the goal quadrant differed across the two contexts. We ran a GLM where we modeled separately the trials in the four quadrants with 4 regressors and applied a parametric modulator to each of them where we modeled the activity evoked by each trial as a function of the angular distance in 60° rotational space from the previously presented trial. This analysis was a modified version of the grid-adaptation analysis employed by Doeller and colleagues [9]: instead of modeling the time passed since the last presentation of a trajectory aligned to 60°, we modeled the angular distance from the previous trial. Given electrophysiological evidence that firing fields of grid-cells increase in number around goal location, we assumed that the grid signal could be higher in the quadrants containing the goals (Q2 in the blue context, Q3 in the green one) compared to those that are far apart from the goal (Q3 in the blue context, Q2 in the green one). We thus defined, through SPM12, contrast weights to give a positive value of + 1 to the grid-modulator for the goal quadrant, -1 for the grid modulator of the quadrant far from the goal, and 0 to the remaining 2 quadrants that had a medium distance (Fig. 4f). Group-level analyses were performed using SPM12.

References

1. Tolman, E.C., 1948. Cognitive maps in rats and men. Psychol. Rev. 55, 189–208.

2. J. O'Keefe, L. Nadel, The Hippocampus as a Cognitive Map (Clarendon, 1978).

3. Bellmund, J.L.S., Gärdenfors, P., Moser, E.I., Doeller, C.F, 2018. Navigating cognition: spatial codes for human thinking. Science 362 80.

4. Behrens, T.E.J., Muller, T.H., Whittington, J.C.R., Mark, S., Baram, A.B., Stachenfeld, K.L., Kurth-Nelson, Z., 2018. What is a cognitive map? Organizing knowledge for flexible behavior. Neuron 100, 490–509.

5. Epstein, R., Patai, E., Julian, J. *et al.* The cognitive map in humans: spatial navigation and beyond. *Nat Neurosci* **20**, 1504–1513 (2017). https://doi.org/10.1038/nn.4656

6. Bottini, R., Doeller, C.F., 2020. Knowledge across reference frames: cognitive maps and im- age spaces. Trends Cogn Sci 24 (8), 606–619. doi:10.1016/j.tics.2020.05.008, PMID: 32586649.

7. J. O'Keefe, J. Dostrovsky, The hippocampus as a spatial map. Preliminary evidence from unit activity in the freely-moving rat. Brain Res. 34, 171–175 (1971).

8. T. Hafting, M. Fyhn, S. Molden, M.-B. Moser, E. I. Moser, Microstructure of a spatial map in the entorhinal cortex. Nature 436, 801–806 (2005). doi: 10.1038/nature03721; pmid: 15965463

9. Doeller, C. F., Barry, C. & Burgess, N. Evidence for grid cells in a human memory network. Nature 463, 657–661 (2010).

10. Morgan, L. K., MacEvoy, S. P., Aguirre, G. K. & Epstein, R. A. Distances between real-world locations are represented in the human hippocampus. J. Neurosci. 31, 1238–1245 (2011).

11. Wolbers T, Wiener JM, Mallot HA, Büchel C. Differential recruitment of the hippocampus, medial prefrontal cortex, and the human motion complex during path integration in humans. J Neurosci. 2007 Aug 29;27(35):9408-16. doi: 10.1523/JNEUROSCI.2146-07.2007. PMID: 17728454; PMCID: PMC6673121.

12. Constantinescu, A. O., O'Reilly, J. X. & Behrens, T. E. J. Organizing conceptual knowledge in humans with a gridlike code. Science 352, 1464–1468 (2016).

13 Theves, S., Fernández, G. & Doeller, C. F. The hippocampus maps concept space, not feature space. J. Neurosci. 40, 7318–7325 (2020).

14. Bao, X. et al. Grid-like neural representations support olfactory navigation of a two-dimensional odor space. Neuron 102, 1066–1075.e5 (2019).

15. Park, S. A., Miller, D. S. & Boorman, E. D. Inferences on a multidimensional social hierarchy use a grid-like code. Nat. Neurosci. 24, 1292–1301 (2021).

16. Viganò S, Rubino V, Soccio AD, Buiatti M, Piazza M. Grid-like and distance codes for representing word meaning in the human brain. Neuroimage. 2021 May 15;232:117876. doi: 10.1016/j.neuroimage.2021.117876. Epub 2021 Feb 24. PMID: 33636346.

17. Viganò S, Rubino V, Buiatti M, Piazza M. The neural representation of absolute direction during mental navigation in conceptual spaces. Commun Biol. 2021 Nov 16;4(1):1294. doi: 10.1038/s42003-021-02806-7. PMID: 34785757; PMCID: PMC8595308.

18. Buzsáki, G., Moser, E. Memory, navigation and theta rhythm in the hippocampal-entorhinal system. Nat Neurosci 16, 130–138 (2013). https://doi.org/10.1038/nn.3304

19. P. Gärdenfors, Conceptual Spaces: The Geometry of Thought (MIT Press, 2000).

20. Burgess N. Spatial memory: how egocentric and allocentric combine. Trends Cogn Sci. 2006 Dec;10(12):551-7. doi: 10.1016/j.tics.2006.10.005. Epub 2006 Oct 30. PMID: 17071127.

21. Byrne P, Becker S, Burgess N. Remembering the past and imagining the future: a neural model of spatial memory and imagery. Psychol Rev. 2007 Apr;114(2):340-75. doi: 10.1037/0033-295X.114.2.340. PMID: 17500630; PMCID: PMC2678675.

22. Andrej Bicanski, Neil Burgess (2018) A neural-level model of spatial memory and imagery eLife 7:e33752 https://doi.org/10.7554/eLife.33752

23. Weniger G, Ruhleder M, Wolf S, Lange C, Irle E. Egocentric memory impaired and allocentric memory intact as assessed by virtual reality in subjects with unilateral parietal cortex lesions. Neuropsychologia. 2009 Jan;47(1):59-69. doi: 10.1016/j.neuropsychologia.2008.08.018. Epub 2008 Aug 22. PMID: 18789955.

24. Bisiach E, Luzzatti C. Unilateral neglect of representational space. Cortex. 1978 Mar;14(1):129-33. doi: 10.1016/s0010-9452(78)80016-1. PMID: 16295118.

25. Aguirre, G. K., & D'Esposito, M. (1999). Topographical disorientation: A synthesis and taxonomy. *Brain: A Journal of Neurology, 122*(9), 1613–1628. https://doi.org/10.1093/brain/122.9.1613

26. Zaehle T, Jordan K, Wüstenberg T, Baudewig J, Dechent P, Mast FW. The neural basis of the egocentric and allocentric spatial frame of reference. Brain Res. 2007 Mar 16;1137(1):92-103. doi: 10.1016/j.brainres.2006.12.044. Epub 2006 Dec 21. PMID: 17258693.

27. Chadwick MJ, Jolly AE, Amos DP, Hassabis D, Spiers HJ. A goal direction signal in the human entorhinal/subicular region. Curr Biol. 2015 Jan 5;25(1):87-92. doi: 10.1016/j.cub.2014.11.001. Epub 2014 Dec 18. PMID: 25532898; PMCID: PMC4291144.

28. Schindler A, Bartels A. Parietal cortex codes for egocentric space beyond the field of view. Curr Biol. 2013 Jan 21;23(2):177-82. doi: 10.1016/j.cub.2012.11.060. Epub 2012 Dec 20. PMID: 23260468.

29. Wolbers T, Hegarty M, Büchel C, Loomis JM. Spatial updating: how the brain keeps track of changing object locations during observer motion. Nat Neurosci. 2008 Oct;11(10):1223-30. doi: 10.1038/nn.2189. Epub 2008 Sep 7. PMID: 18776895.

30. Stein JF. Representation of egocentric space in the posterior parietal cortex. Q J Exp Physiol. 1989 Sep;74(5):583-606. doi: 10.1113/expphysiol.1989.sp003314. PMID: 2687924.

31. Wilber AA, Clark BJ, Forster TC, Tatsuno M, McNaughton BL. Interaction of egocentric and world-centered reference frames in the rat posterior parietal cortex. J Neurosci. 2014 Apr 16;34(16):5431-46. doi: 10.1523/JNEUROSCI.0511-14.2014. PMID: 24741034; PMCID: PMC3988403.

32. Nyberg N, Duvelle É, Barry C, Spiers HJ. Spatial goal coding in the hippocampal formation. Neuron. 2022 Feb 2;110(3):394-422. doi: 10.1016/j.neuron.2021.12.012. Epub 2022 Jan 14. PMID: 35032426.

33. Boccara CN, Nardin M, Stella F, O'Neill J, Csicsvari J. The entorhinal cognitive map is attracted to goals. Science. 2019 Mar 29;363(6434):1443-1447. doi: 10.1126/science.aav4837. PMID: 30923221.

34. Butler WN, Hardcastle K, Giocomo LM. Remembered reward locations restructure entorhinal spatial maps. Science. 2019 Mar 29;363(6434):1447-1452. doi: 10.1126/science.aav5297. PMID: 30923222; PMCID: PMC6516752.

35. Frey M, Nau M, Doeller CF. Magnetic resonance-based eye tracking using deep neural networks. Nat Neurosci. 2021 Dec;24(12):1772-1779. doi: 10.1038/s41593-021-00947-w. Epub 2021 Nov 8. PMID: 34750593.

36. Nau M, Schindler A, Bartels A. Real-motion signals in human early visual cortex. Neuroimage. 2018 Jul 15;175:379-387. doi: 10.1016/j.neuroimage.2018.04.012. Epub 2018 Apr 10. PMID: 29649561.;

37. Polti I, Nau M, Kaplan R, van Wassenhove V, Doeller CF. Rapid encoding of task regularities in the human hippocampus guides sensorimotor timing. Elife. 2022 Nov 1;11:e79027. doi: 10.7554/eLife.79027. PMID: 36317500; PMCID: PMC9625083.;

38. Nau M, Navarro Schröder T, Bellmund JLS, Doeller CF. Hexadirectional coding of visual space in human entorhinal cortex. Nat Neurosci. 2018 Feb;21(2):188-190. doi: 10.1038/s41593-017-0050-8. Epub 2018 Jan 8. PMID: 29311746.

39. Shelton, A.L., McNamara, T.P. Spatial memory and perspective taking. *Memory & Cognition* **32**, 416–426 (2004). https://doi.org/10.3758/BF03195835

40. Shepard RN, Metzler J. Mental rotation of three-dimensional objects. Science. 1971 Feb 19;171(3972):701-3. doi: 10.1126/science.171.3972.701. PMID: 5540314.

41. Zacks JM. Neuroimaging studies of mental rotation: a meta-analysis and review. J Cogn Neurosci. 2008 Jan;20(1):1-19. doi: 10.1162/jocn.2008.20013. PMID: 17919082.

42. Harris IM, Miniussi C. Parietal lobe contribution to mental rotation demonstrated with rTMS. J Cogn Neurosci. 2003 Apr 1;15(3):315-23. doi: 10.1162/089892903321593054. PMID: 12729485.

43. Bellmund JL, Deuker L, Navarro Schröder T, Doeller CF. Grid-cell representations in mental simulation. Elife. 2016 Aug 30;5:e17089. doi: 10.7554/eLife.17089. PMID: 27572056; PMCID: PMC5005038.

44. Binder JR, Desai RH, Graves WW, Conant LL. Where is the semantic system? A critical review and meta-analysis of 120 functional neuroimaging studies. Cereb Cortex. 2009 Dec;19(12):2767-96. doi: 10.1093/cercor/bhp055. Epub 2009 Mar 27. PMID: 19329570; PMCID: PMC2774390.

45. Svoboda E, McKinnon MC, Levine B. The functional neuroanatomy of autobiographical memory: a meta-analysis. Neuropsychologia. 2006;44(12):2189-208. doi: 10.1016/j.neuropsychologia.2006.05.023. Epub 2006 Jun 27. PMID: 16806314; PMCID: PMC1995661.

46. Parkinson, C. et al. (2014) A common cortical metric for spatial, temporal, and social distance. J. Neurosci. 34, 1979–1987

47. Peer, M. et al. (2015) Brain system for mental orientation in space, time, and person. Proc. Natl. Acad. Sci. 112, 11072–11077

48. Tavares, R.M. et al. (2015) A map for social navigation in the human brain. Neuron 87, 231–243

49. Arzy S, Schacter DL. Self-Agency and Self-Ownership in Cognitive Mapping. Trends Cogn Sci. 2019 Jun;23(6):476-487. doi: 10.1016/j.tics.2019.04.003. Epub 2019 May 4. PMID: 31064702; PMCID: PMC6584024.

50. van Wijngaarden JB, Babl SS, Ito HT. Entorhinal-retrosplenial circuits for allocentric-egocentric transformation of boundary coding. Elife. 2020 Nov 3;9:e59816. doi: 10.7554/eLife.59816. PMID: 33138915; PMCID: PMC7609058.

51. Oosterhof NN, Connolly AC, Haxby JV. CoSMoMVPA: Multi-Modal Multivariate Pattern Analysis of Neuroimaging Data in Matlab/GNU Octave. Front Neuroinform. 2016 Jul 22;10:27. doi: 10.3389/fninf.2016.00027. PMID: 27499741; PMCID: PMC4956688.

52. Maass, A., Berron, D., Libby, L.A., Ranganath, C., Düzel, E., 2015. Functional subregions of the human entorhinal cortex. Elife 4, 1–20.

53. Northoff G, Heinzel A, de Greck M, Bermpohl F, Dobrowolny H, Panksepp J. Self-referential processing in our brain--a meta-analysis of imaging studies on the self. Neuroimage. 2006 May 15;31(1):440-57. doi: 10.1016/j.neuroimage.2005.12.002. Epub 2006 Feb 7. PMID: 16466680.

54. PS Muhle-Karbe, H Sheahan, G Pezzulo, HJ Spiers, S Chien, NW Schuck, CSummerfield (2023) Goal-seeking compresses neural codes for space in the human hippocampus and orbitofrontal cortex. bioRxiv

Acknowledgments

Supplementary Materials
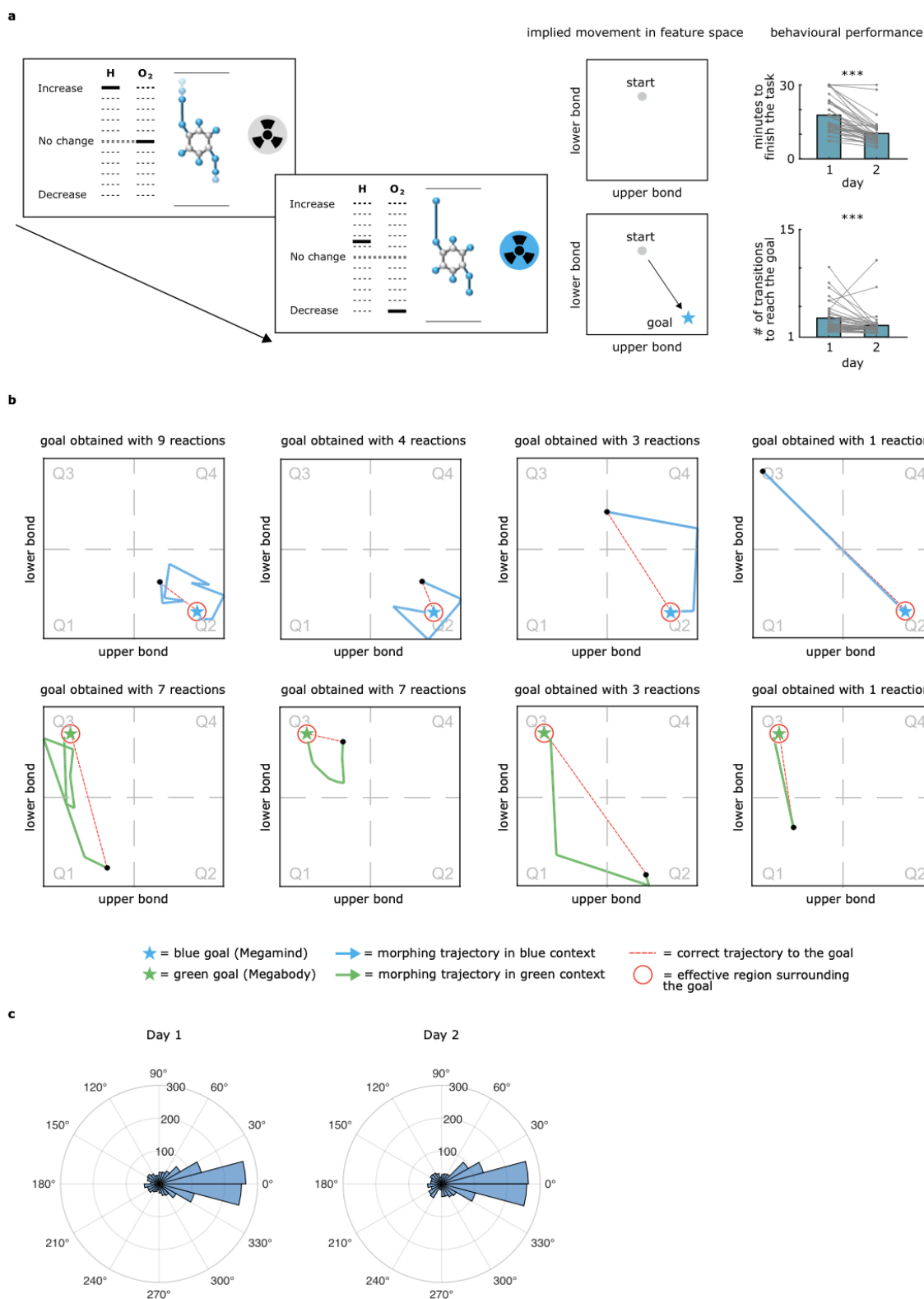
Supplementary Fig. 1 | Collect task with hint (training). a, During the first training task ("Collect task with hint", see Methods) participants actively modified the aspect ratio of a wrong molecule to match the respective conceptual goal. Visual feedback (the hint) signaled when the correct configuration was reached and when the participant could "collect" the molecule to proceed to the next trial. Almost all of the participants (35/40, 87.5%) collected all the required molecules (20 blue, 20 green) within the time limit of 30 minutes on the first day already

(mean time on day 1 = 17.7 min, std = 7.05 min) and significantly improved their performance on the next day, as indicated both by the time taken to finish the task (mean time on day 2 = 10.3 min, std = 5.24 min; mean differential time day 2 - day 1 = -7.42 min, std = 5.43 min; z-score = -5.37, p = < 0.001, Wilcoxon sign rank test) and by the number of transitions necessary to reach the goal (mean number of transitions on day 1 = 3.49, std = 1.91; on day 2 = 2.55, std = 1.69; mean difference between days = -0.94, std = 2.18; z-score = -3.98, p = < 0.001, Wilcoxon sign rank test; perfect performance: 1 transition). **b,** Examples of the implied trajectories navigated by participants in the 2D feature spaces. On some trials (left) they tried many reactions/trajectories before finding the goal, while on other trials they reached it more directly (right). **c**, Distribution of all the first trajectories taken by participants during the Collect Task, expressed as error from the perfect trajectory to the goal. A value of 0° would indicate a perfect performance, a value of 180° would indicate navigation in the opposite direction.
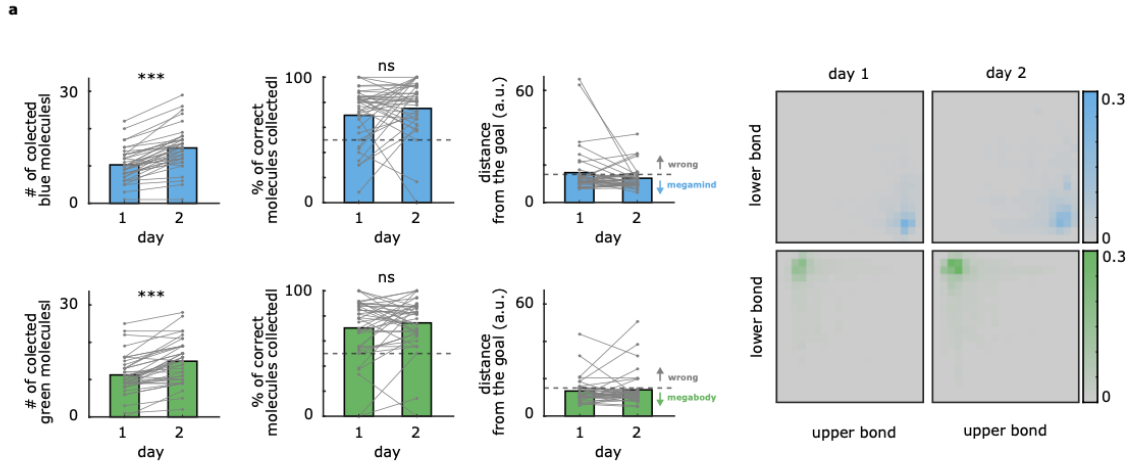
Supplementary Fig. 2 | Collect task without hint (training). a, During the second task ("Collect task without hint", see Methods) participants followed the same procedure of the previous task but now i) they didn't have any visual feedback, ii) they could also collect wrong molecules (that would count as mistakes), and iii) they had only 3 minutes per color context to collect as many correct molecules as they could. Results indicated that i) participants collected more molecules on day 2 compared to day 1 (mean increment blue molecule = 4.52 corresponding to 43.9% with respect to day 1 (std = 2.74); z-score = 5.37, p < 0.001, Wilcoxon sign rank test - mean increment green molecule = 3.68 corresponding to 32.7% with respect to day 1 (std = 3.14); z-score = 4.99, p < 0.001, Wilcoxon sign rank test), ii) the percentage of correct molecules was >=70% on both days (p > .10), and iii) that, on average, they collected molecules at short distances from the goal locations (mean distance from the goal on day 2 = 12.9 a.u. (std = 6.06) and 14.04 a.u. (std = 8.94) for the blue and green molecule respectively, with 32/40 participants (80%) having an average distance from the goal below the correct threshold of 15 a.u. for both molecules).
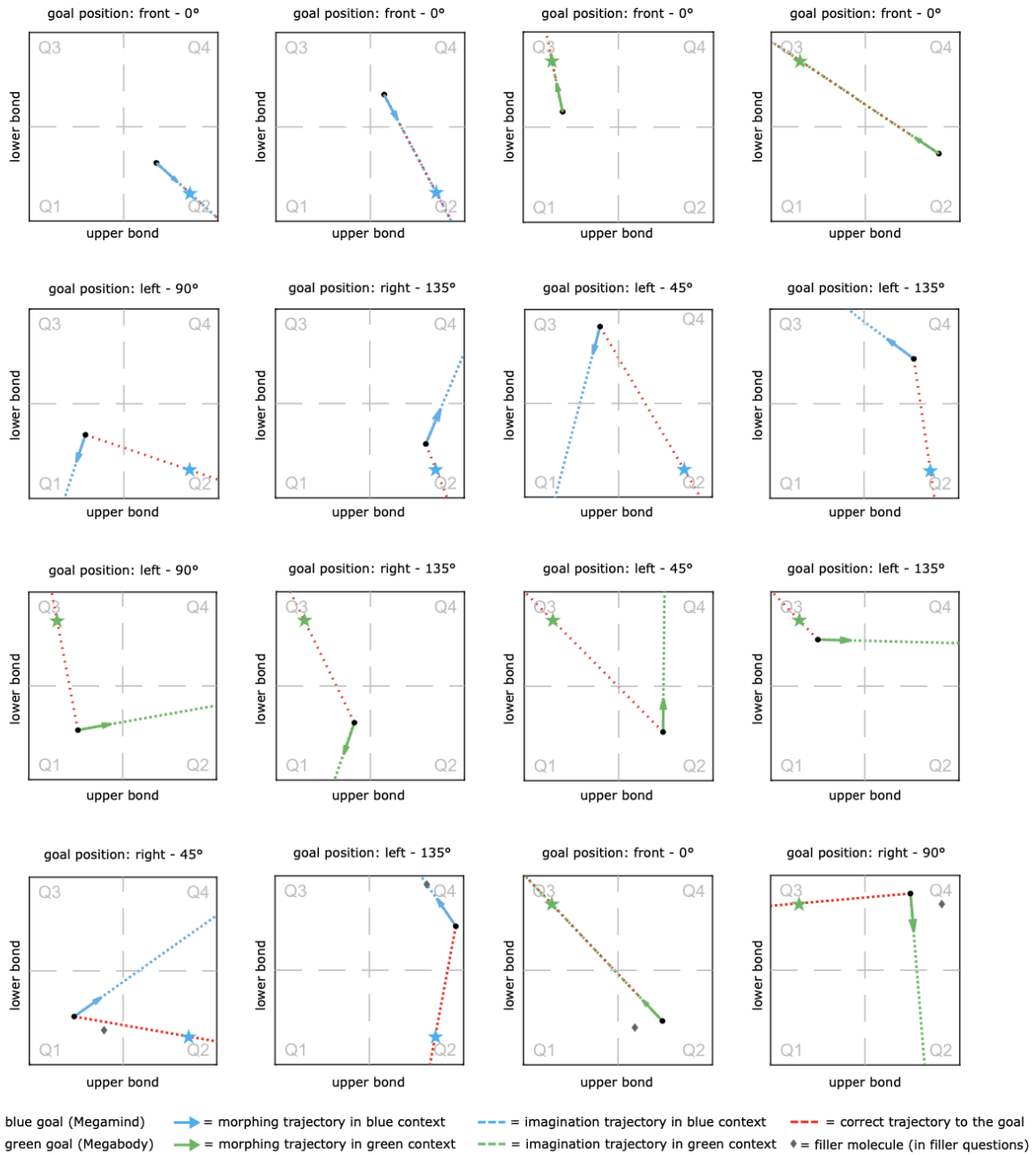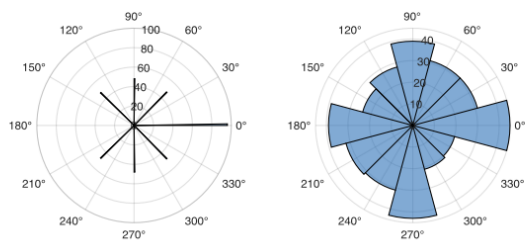
Supplementary Fig. 3 | Example trajectories in the Recall task (training + fMRI). a, Participants were presented with random wrong molecules that started morphing (solid arrow) and they were instructed to imagine the morphing to continue in the same way (blue or green dashed line). They were asked to indicate whether the morphing would result in the correct configuration or not: the correct trajectory that would lead to the goal is indicated as a red dashed line. When the blue/green and the red dashed lines overlap, it means that this is a trajectory directed to the goal (on-target trial) and participants are expected to respond "Yes". When they do not overlap, they are expected to respond "No" (off-target trials). Off-target trials could miss the goal at various "egocentric-like conditions": 135° to the left, 90° to the left, 45° to the left, 45° to the right, 90° to the right, 135° to the right (see Main Text and Methods). **b,** Distribution of the sampled directions for egocentric conditions (left) and allocentric conditions (right). Egocentric directions are referenced to the target direction to the goal (0°), while allocentric conditions are referenced to the horizontal axis (0°).
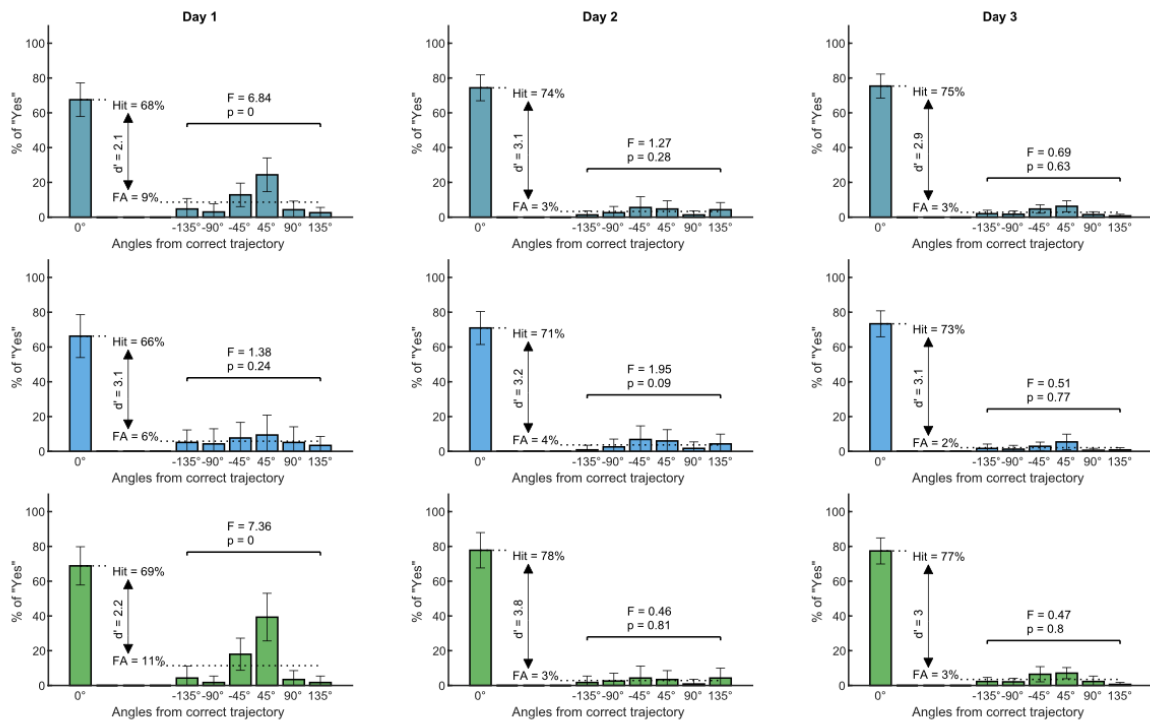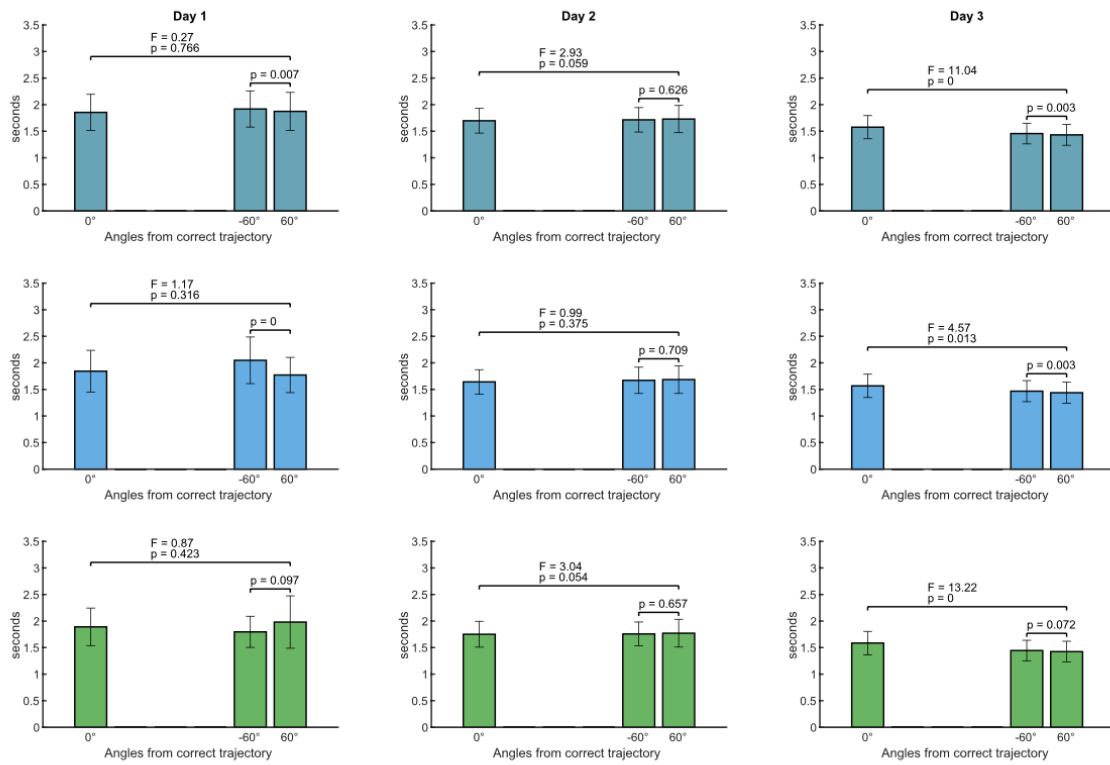
Supplementary Fig. 4 | Performance in the Recall task across the 3 days of experiment - Accuracy in the target question. a, For each day, we report the % of "Yes" responses as a function of the egocentric-like angular condition. 0° refers to on-target trials, and the % of Yes judgments here corresponds to the Hit rate. The average of the % of Yes judgments for the other conditions (-135°, -90°, etc) corresponds to the False Alarm (FA) rate. These two values are also used to compute a summary measure of the sensitivity to the correct trajectories (d'). An F-test is computed on the off-target conditions to verify whether any of them is significantly different from the others, which doesn't seem to be the case on day 3, during the fMRI scanning day. The first row indicates the performance when the two context/molecules are averaged, while the second and the third shows performance for the blue and green context, respectively. p = 0 indicates p <.001
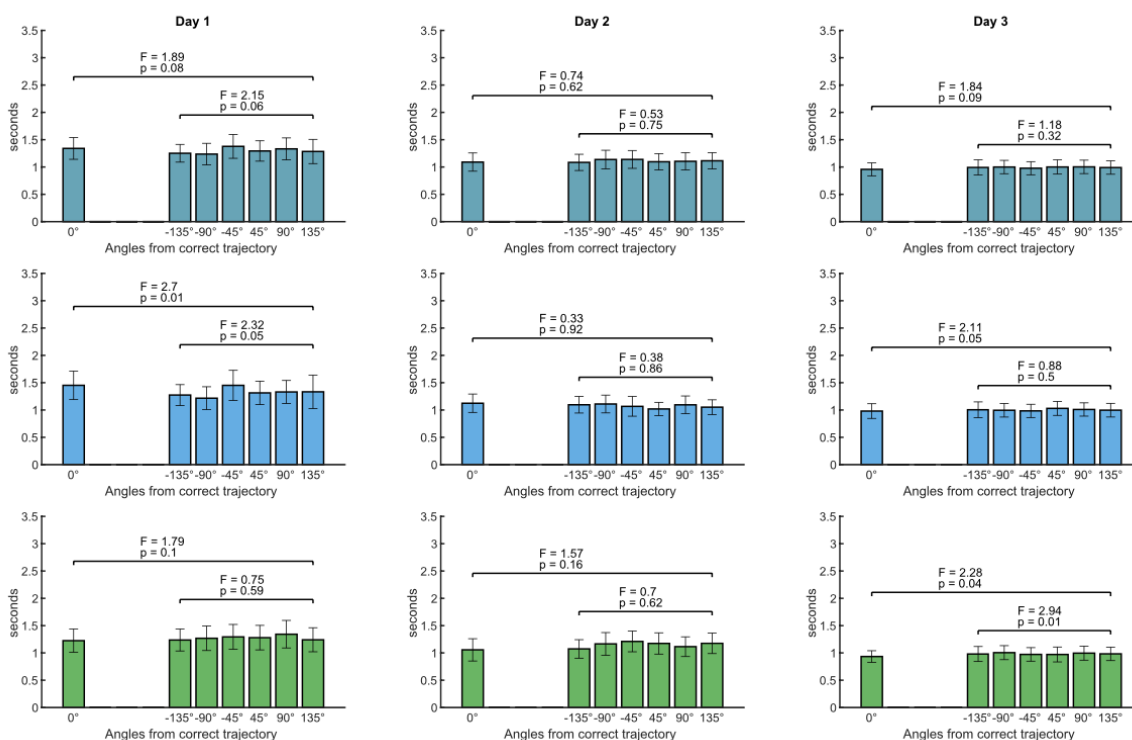
Supplementary Fig. 5 | Performance in the Recall task across the 3 days of experiment - Reaction Times in the target question. a, For each day, we report the Reaction Times (RTs) of the responses as a function of the egocentric-like angular condition. 0° refers to on-target trials. An F-test is computed both on all trials and on the off-target conditions solely to verify whether any of them is significantly different from the others. The first row indicates the performance when the two context/molecules are averaged, while the second and the third shows performance for the blue and green context, respectively.
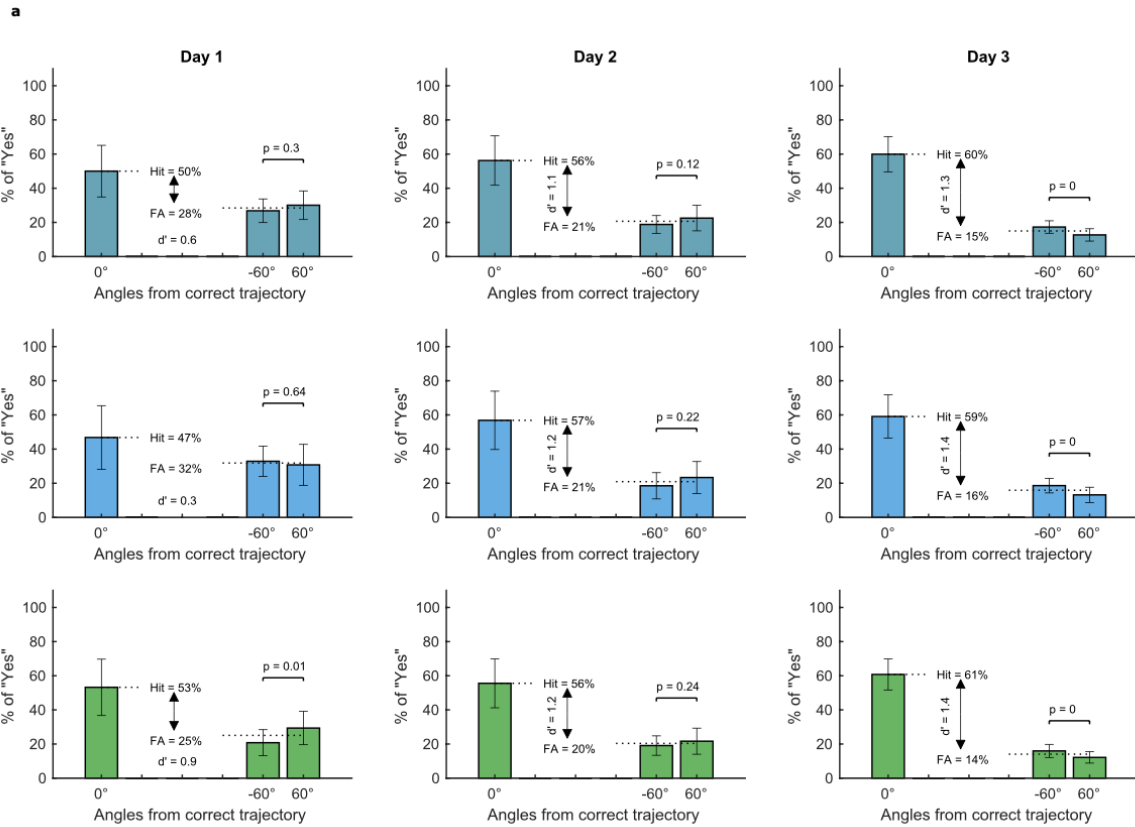
Supplementary Fig. 6 | Performance in the Recall task across the 3 days of experiment - Accuracy in the filler question. a, For each day, we report the % of "Yes" responses as a function of the angular trajectory from the filler goal (see Main text and Methods). 0° refers to on-target trials. The statistics reported correspond to those in Supplementary Fig. 4, adapted to the details of this question. We observed an interesting bias consisting of higher accuracy for "filler off-target trials" for one of the two off-target trajectories. This effect is unlikely to reflect an alteration of the global map and we cannot offer any conclusive interpretation of it, although it is worth noting that for one of the two contexts (green one, last row), this "side preference" was in the opposite direction on the first day, and it changed on the 3rd one to match the same direction of the blue context (second row). A potential interpretation is that this behavioral effect reflects the realignment of the two spaces into one via mental rotation, suggesting for instance that it was the green context, on average, that was rotated, but this remains highly speculative at the moment and should be taken into account with caution.

Supplementary Fig. 7 | Performance in the Recall task across the 3 days of experiment - Reaction Times in the filler question. a, For each day, we report the Reaction times (RTs) of the responses as a function of the angular trajectory from the filler goal (see Main text and Methods). 0° refers to "on-target filler trials".
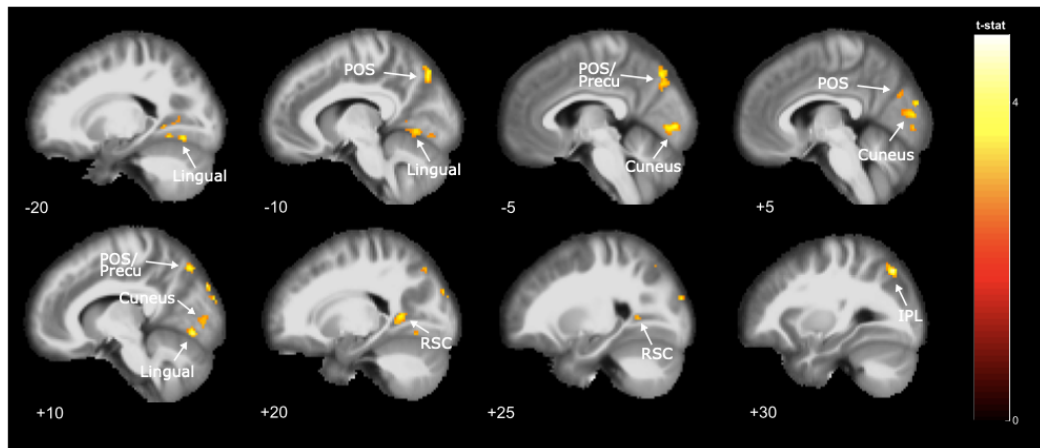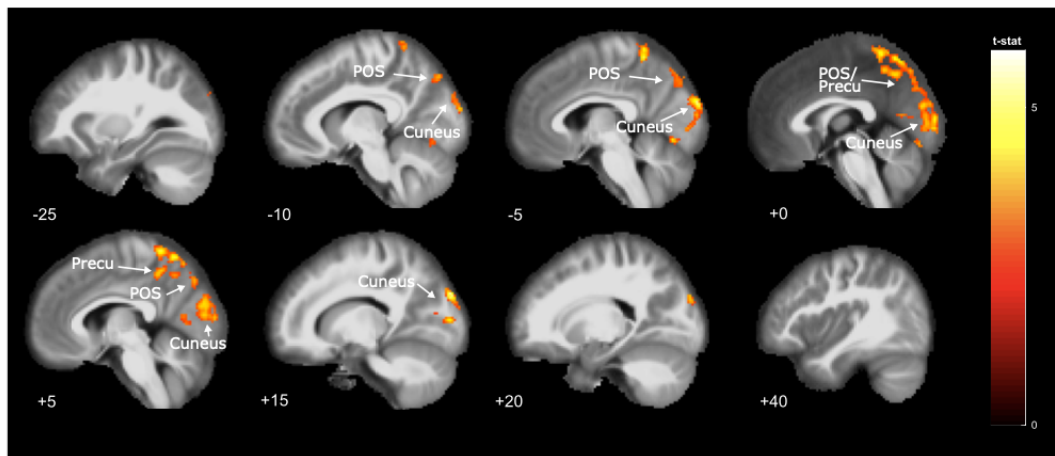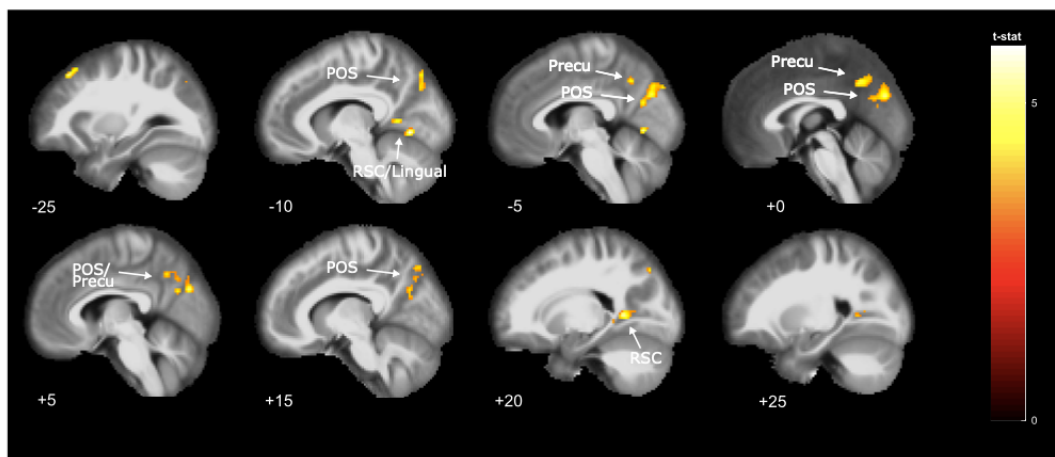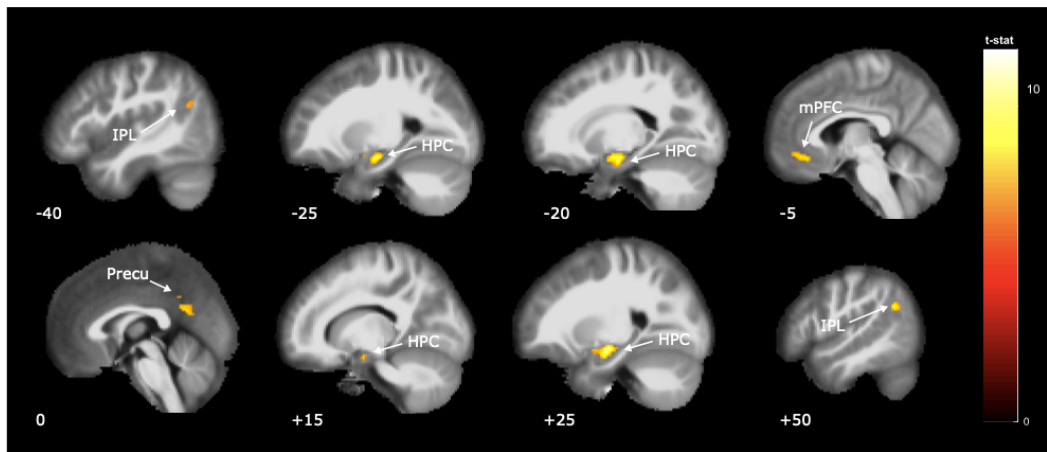
Supplementary Fig. 8 | Whole-brain adaptation effect of egocentric-like conditions without on-target trials. a, As a control, we repeated the main analysis reported in Fig. 2b-c but now focusing only on off-target trials, thus excluding those trajectories that were directed to the goal, revealing that the effect was still present and thus it was not dependent on on-target trials. Statistical maps are thresholded at p<.001 at voxel level, and corrected for multiple comparisons at cluster level with p<.05. Significant clusters were found in parieto-occipital sulcus (-8 -78 44), lingual gyrus (16 -72 -8), cuneus (-4 -86 -2), retrosplenial cortex (16 -44 -2), and inferior parietal lobule (30 -72 48).
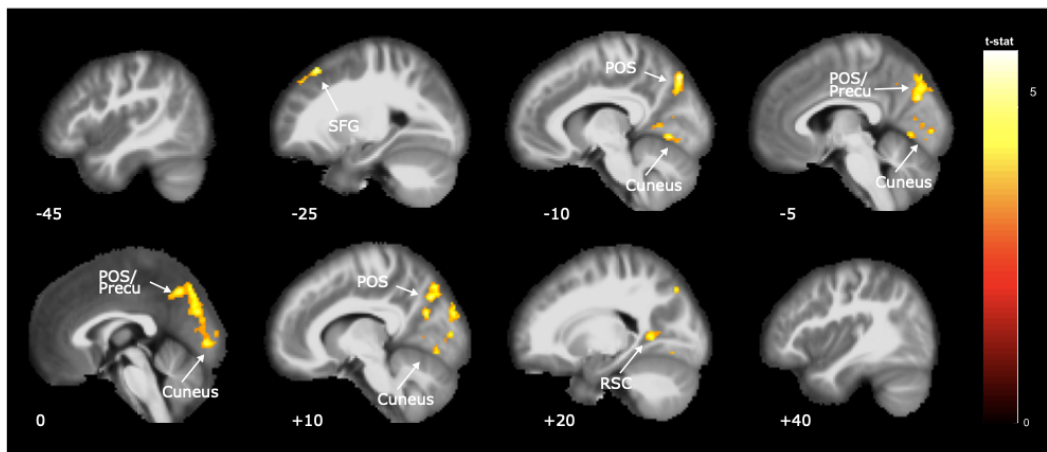
Supplementary Fig. 9 | Whole-brain adaptation effect of egocentric-like conditions for the two contexts separately. a, As a control, we repeated the main analysis reported in Fig. 2b-c but now focusing on the two contexts separately,, revealing that the effect was still present and thus it was not dependent on one specific molecule. Statistical maps are thresholded at p<.001 at voxel level, and corrected for multiple comparisons at cluster level with p<.05. Significant clusters were found in the cuneus (14 -92 30) and precuneus/PCC (-4 -50 70 and 2 -50 52) for the blue context, and in the POS (-4 -78 30), retrosplenial cortex (-10 -58 6), superior frontal gyrus (-28 30 52), lingual gyrus (-8 -70 -4) for the green context.
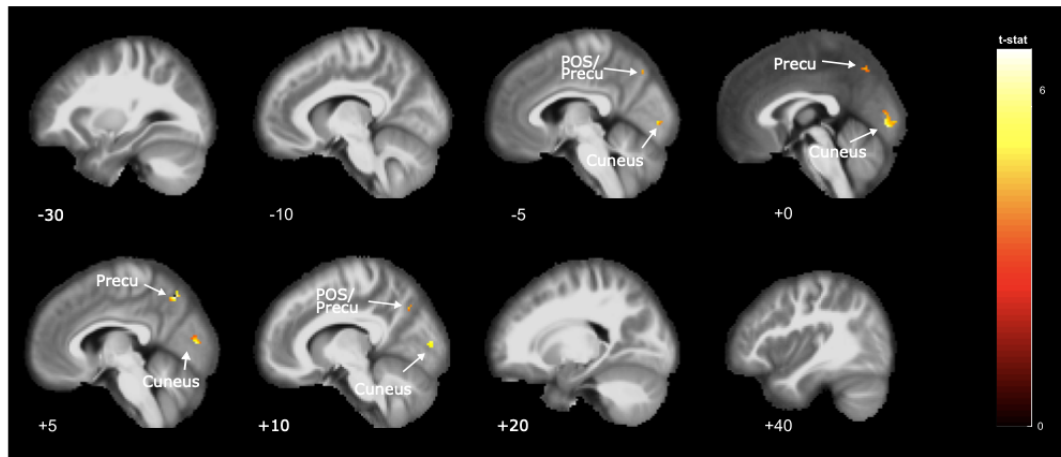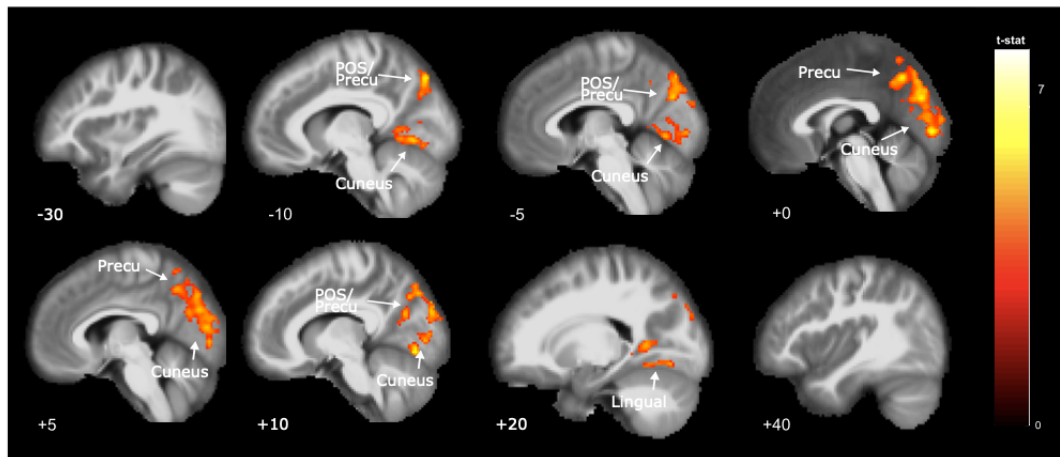
Supplementary Fig. 10 | Whole-brain adaptation effect of egocentric-like conditions after controlling for distance. As a control analysis, we repeated the main analysis reported in Fig. 2b-c after controlling for the distance to the goal. We reasoned that egocentric-like conditions, in principle, convey information about the relative distance to the goal, namely whether (and how much) we are getting closer to the goal or not. We created an additional parametric modulator modeling this information for each trial, which, across runs and subjects, was poorly correlated with our main regressor for egocentric-like conditions (Pearson's r = 0.10). Nevertheless, to provide conclusive evidence that the egocentric-like effect was independent of the distance effect, we put both the parametric modulators in the same GLM, looking for adaptation to the egocentric-like conditions after controlling/excluding the brain activity modulated by distance. Whole-brain results for the distance modulator and the controlled egocentric-like modulator are reported in **a** and **b**, respectively. Statistical maps are thresholded at p<.001 at voxel level, and corrected for multiple comparisons at cluster level with p<.05. Significant clusters were found in the bilateral hippocampi (24 -12 -16 and -24 -14 -18), bilateral inferior parietal lobules (48 -58 30 and -44 -64 24), precuneus (0 -58 24) and medial prefrontal cortex (-6 36 -14) for distance effect, and in the POS/precuneus (-12 -80 48), superior frontal gyrus (-28 28 54), cuneus (8 -78 6) and bilateral retrosplenial cortices/lingua gyrus (-18 -60 2 and 20 -54 4) for the egocentric effect.
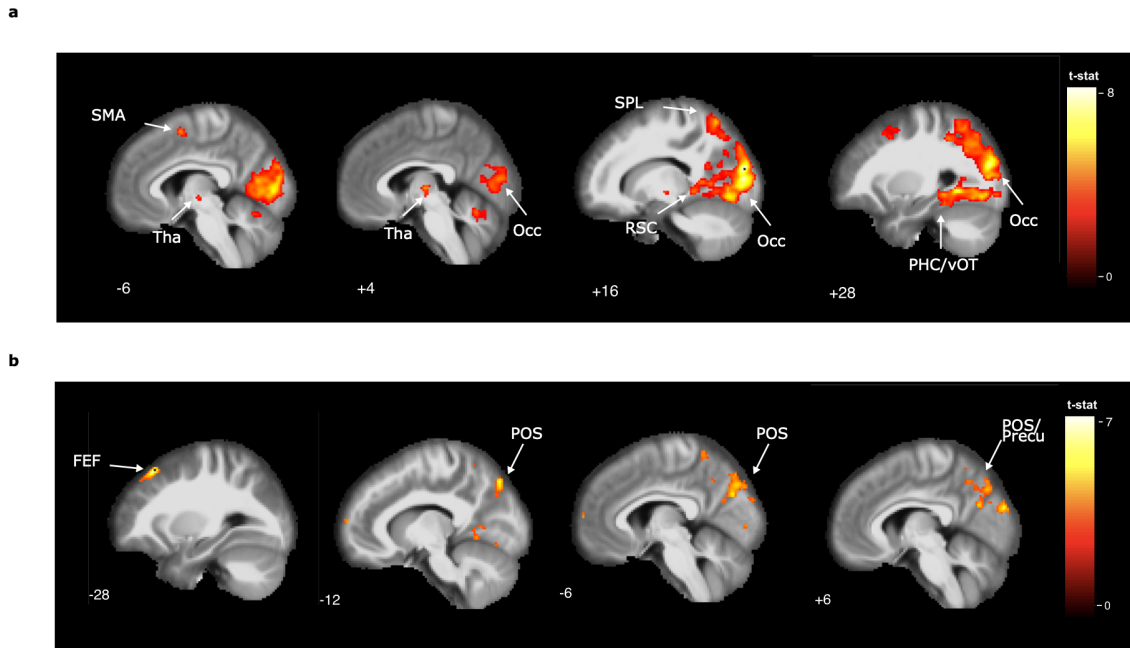
Supplementary Fig. 11 | Whole-brain adaptation effect of "left" vs "right" egocentric-like conditions. a, As a control, we repeated the main analysis reported in Fig. 2b-c but now modeling the (log) time since the last presentation of a trajectory that had the goal on one side (left or right), irrespective of the magnitude of the angle (if 45°, 90°, or 135°). Results indicate a significant cluster in the POS territory (p<.001 corrected at cluster level), although an ROI control reveals that this effect was significantly stronger in our main analysis (mean difference with the main effect = 0.37, std = 0.92, z-score = 2.5, p < 0.05, Wilcoxon sign rank test), when we modeled both the side (left vs right) and the angular magnitude (45°, 90°, 135°), suggesting that this brain region is associated with a fine-graded code of egocentric-like conditions. Statistical maps are thresholded at p<.001 at voxel level, and corrected for multiple comparisons at cluster level with p<.05. Significant clusters were found in the precuneus (4 -66 52) and in the cuneus (14 -86 4).

Supplementary Fig. 12 | Whole-brain adaptation effect of egocentric-like conditions after controlling for starting position. Starting positions were selected pseudo-randomly across the experiment, being balanced across the four quadrants. This makes it unlikely that our main effect of egocentric-like responses could be explained by repetition of the starting position. Nevertheless, as a further control, we ran an additional analysis to verify that this was the case: our main regressor of interest modeling egocentric conditions was put after a control regressor modeling the (log) time since the last presentation of a trajectory that started in a specific quadrant. Whole-brain analysis revealed very similar results to our main analysis after controlling for and excluding the variance explained by this potentially confounding variable (that is, working on its residuals). Statistical maps are thresholded at p<.001 at voxel level, and corrected for multiple comparisons at cluster level with p<.05. Significant clusters were found in the cuneus (0 -88 -2), retrosplenial cortex/lingual gyrus (16 -56 4), POS/precuneus (-4 -78 32), precuneus (-8 -54 64).

Supplementary Fig. 13 | Whole-brain adaptation effect of egocentric-like conditions after controlling for allocentric head-direction like conditions. a, Allocentric directions were resampled with a granularity of 30°, to allow a proper implementation of the time-dependent adaptation analysis and for consistency with the grid-like analysis (see Figure 4). The resulting clusters reveal similarities with previous findings of allocentric head-direction like coding during virtual reality fMRI experiments, e.g., Doeller et al. 2010 and Shine et al. 2015, specially for what concerns the RSC and the Thalamus (Tha). **b**, adaptation of egocentric like conditions after controlling for allocentric effects. Statistical maps are thresholded at p<.001 at voxel level, and corrected for multiple comparisons at cluster level with p<.05. Significant clusters were found in the occipital lobe (16 -90 18), thalamus (14 -14 2), parahippocampus (32 -26 -20) for the allocentric "head direction like" effect, and in the superior frontal gyrus/frontal eye fields (-28 28 54), precuneus/POS (-12 -80 48), and retrosplenial cortex (-18 60 2) for the egocentric effect.
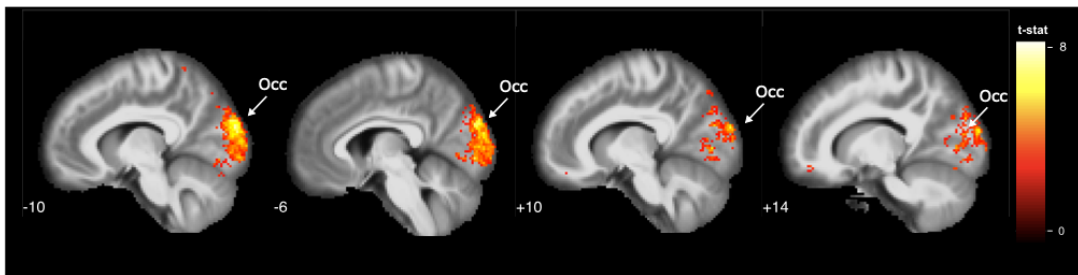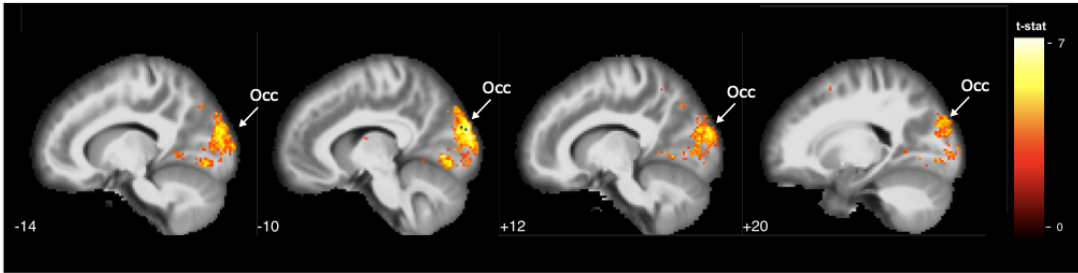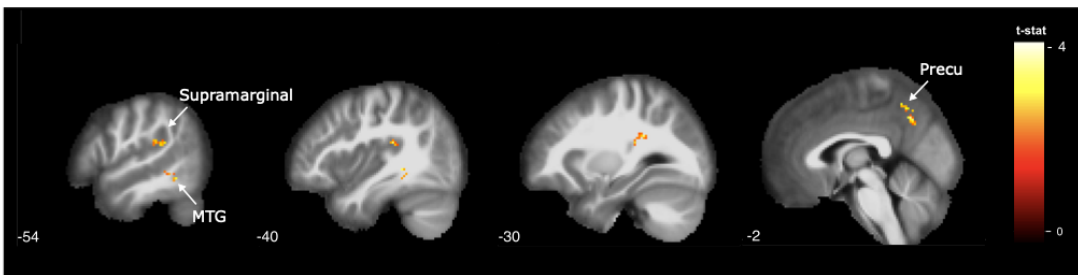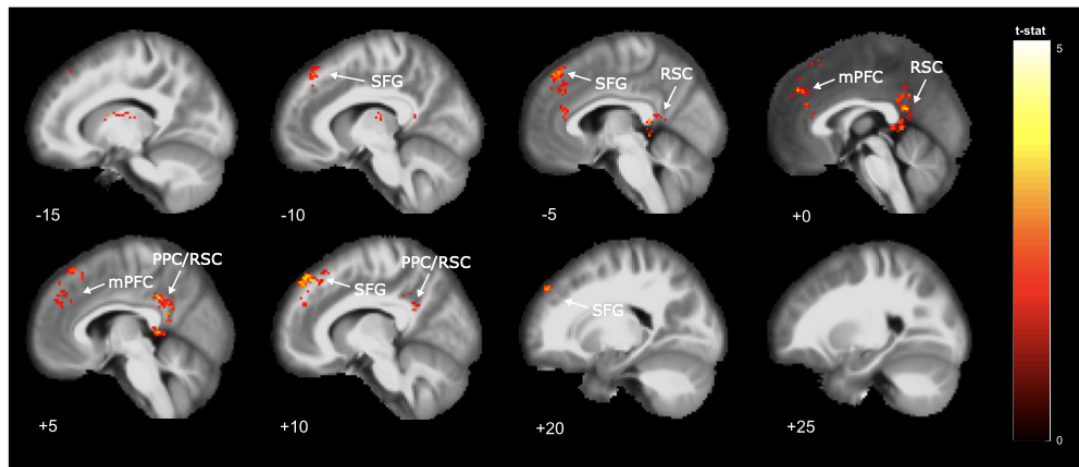
Supplementary Fig. 14 | Whole brain decoding of egocentric conditions within contexts over the cross-context decoding a-b, within context decoding of egocentric conditions reveals significantly stronger clusters in the occipital cortex compared to the cross context decoding. Statistical maps are thresholded at p<.001 at voxel level, and corrected for multiple comparisons at cluster level with p<.05. Significantly stronger clusters were found in the occipital cortex when we compared within context vs cross context decoding (-8 -94 26 and -10 -96 22 respectively for blue>cross and green>cross). **c,** Significantly stronger clusters were found in the precuneus (-2 -60 42), supramarginal gyrus (-48 -32 22), and MTG (-40 -40 -4) when we compared cross context decoding vs blue context decoding with a threshold of p<.01 at voxel level, corrected for multiple comparisons at voxel level with p<.05.. No statistically significant clusters were obtained for the contrast cross context decoding vs green context decoding.
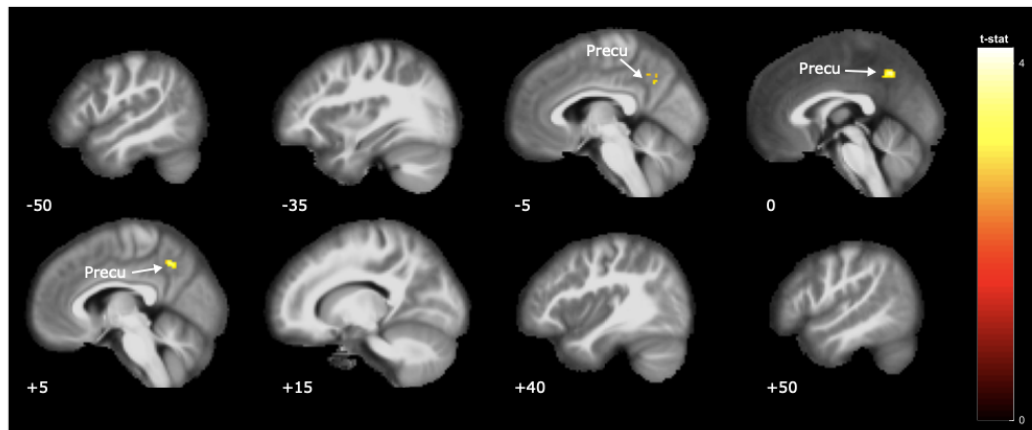
a

Supplementary Fig. 15 | Whole-brain decoding analysis without on-target trials. a, As a control analysis, we repeated the main analysis reported in Fig. 2d-e but now focusing only on off-target trials, thus excluding those trajectories that were directed to the goal, revealing that the effect was still present, although weaker, and thus it was not completely dependent on on-target trials. Statistical maps are thresholded at p<.05 at voxel level, and corrected for multiple comparisons at cluster level with p<.05. Significant clusters were obtained in the superior frontal gyrus/frontal eye field (14 48 44) and posterior parietal cortex extending in the retrosplenial cortex (2 -48 20).

a

Supplementary Fig. 16 | Whole-brain representational similarity analysis for mental rotation without goal quadrants. a, As a control analysis, we repeated the main analysis reported in Fig. 3a-b but now focusing only on quadrants that did not contain the goal, thus excluding Q2-blue and Q3-green. Results revealed that the effect in precuneus (-2 -56 44) was still significant (p<.005 at voxel level, corrected for multiple comparisons at cluster level with p<.05), thus indicating that this region was not simply representing cross-context correspondence of goal quadrants.

Region	Extent (voxels)	p (corr.)	p (uncorr.)	t-stat	x	y	z
Medial Occipito-Parietal Cortex/POS	1539	<.001	<.001	5.83	6	-92	22
	1539		<.001	5.68	-12	-80	48
	1539		<.001	5.67	-4	-76	30
Lingual gyrus	168	<.001	<.001	5.61	-8	-70	-4
Superior frontal gyrus/FEF	126	<.001	<.001	6.89	-28	28	54
Cuneus	83	0.001	<.001	4.29	20	-54	4
Precuneus	73	0.002	<.001	4.27	-8	-54	64

Table 1 | Cluster (and sub-cluster) peaks of the whole-brain adaptation analysis for egocentric-like conditions reported in Fig. 2c. p (uncorr.) = uncorreced p-value at voxel level; p (corr.) = p-value corrected for multiple comparisons at cluster level; x,y,z coordinates are in MNI space.

Region	Extent (voxels)	p (corr.)	p (uncorr.)	t-stat	x	y	z
Right Inferior Parietal Lobule	92	0.003	<.001	4.9	36	-56	42
Precuneus	72	0.005	<.001	4.51	-2	-56	46
Left Inferior Parietal Lobule	69	0.005	<.001	4.93	-32	-62	40

Table 2 | Cluster peaks of the whole-brain quadrant-by-quadrant similarity analysis (rotation effect) reported in Fig. 3b. p (uncorr.) = uncorreced p-value at voxel level; p (corr.) = p-value corrected for multiple comparisons at cluster level; x,y,z coordinates are in MNI space.

Region	Extent (voxels)	p (corr.)	p (uncorr.)	t-stat	x	y	z
Superior Parietal Lobule	293	<.001	<.001	5.18	-30	-46	66
Medial Prefrontal Cortex	112	0.001	<.001	4.46	2	48	-2
Left Angular Gyrus	75	0.004	<.001	4.19	-50	-70	18
Entorhinal Cortex	8	0.01	<.001	4.23	16	-6	-26

Table 3 | Cluster peaks of the whole-brain analysis on the alteration of the grid-like signal reported in Fig. 4g. p (uncorr.) = uncorreced p-value at voxel level; p (corr.) = p-value corrected for multiple comparisons at cluster level; x,y,z coordinates are in MNI space.